DEEP LEARNING-BASED CLASSIFICATION OF BREAST TUMORS IN ULTRASOUND IMAGES

AYUB AHMED OMAR

DEPARTMENT OF BIOMEDICAL ENGINEERING
UNIVERSITY OF MALAYA
KUALA LUMPUR

2022

DEEP LEARNING-BASED CLASSIFICATION OF BREAST TUMORS IN ULTRASOUND IMAGES

AYUB AHMED OMAR

RESEARCH REPORT SUBMITTED IN FULFILMENT OF THE REQUIREMENTS FOR THE DEGREE OF MASTER OF BIOMEDICAL ENGINEERING

DEPARTMENT OF BIOMEDICAL ENGINEERING
UNIVERSITY OF MALAYA
KUALA LUMPUR

2022

UNIVERSITY OF MALAYA

ORIGINAL LITERARY WORK DECLARATION

Name of Candidate:Ayub Ahmed Omar

Matric No: S2016803

Name of Degree: Master of Biomedical Engineering

Title of Project Paper/Research Report/Dissertation/Thesis ("this Work"): Deep Learning-Based Classification of Breast Tumors in Ultrasound Images

Field of Study: Biomedical Engineering

I do solemnly and sincerely declare that:

(1) I am the sole author/writer of this Work;
(2) This Work is original;
(3) Any use of any work in which copyright exists was done by way of fair dealing and for permitted purposes and any excerpt or extract from, or reference to or reproduction of any copyright work has been disclosed expressly and sufficiently and the title of the Work and its authorship have been acknowledged in this Work;
(4) I do not have any actual knowledge nor do I ought reasonably to know that the making of this work constitutes an infringement of any copyright work;
(5) I hereby assign all and every rights in the copyright to this Work to the University of Malaya ("UM"), who henceforth shall be owner of the copyright in this Work and that any reproduction or use in any form or by any means whatsoever is prohibited without the written consent of UM having been first had and obtained;
(6) I am fully aware that if in the course of making this Work I have infringed any copyright whether intentionally or otherwise, I may be subject to legal action or any other action as may be determined by UM.

Candidate's Signature Date: 16/06/2022

Subscribed and solemnly declared before,

Witness's Signature Date:

Name:

Designation

DEEP LEARNING-BASED CLASSIFICATION OF BREAST TUMORS IN ULTRASOUND IMAGES

ABSTRACT

The use of ultrasound imaging techniques to diagnose breast cancer at an early stage is a popular and effective method. The issue with traditional breast ultrasound diagnosis is that, unlike magnetic resonance imaging (MRI) and mammography, it is prone to making a mistake due to its subjectivity, which could result in a missed diagnosis and an unnecessary biopsy. In this research project, recent breast tumor classification model algorithms are investigated and analyzed, and then the limitations and gaps in previous techniques are highlighted. The Breast Ultrasound Images Dataset (BUID) has been prepared and preprocessed in order to train both the U-Net and Convolutional neural network (CNN) classifier models. The U-Net model is used to locate tumor growth in original medical images because of its capacity to do classification on each pixel in the input image and produce input and output images that are the same size. Then, a CNN classifier model is built to classify the U-Net model's generated mask images as benign, malignant, or normal. The accuracy performance matrices and Dice loss function are used to evaluate the performance of both U-Net and CNN classifier models. The U-Net model have achieved an accuracy of 93% and a dice loss value of 0.4391. Whereas the CNN classifier model has achieved an accuracy of 85%.

Keywords: Breast ultrasound image, Convolutional neural networks, mass classification.

KLASIFIKASI BERASASKAN PEMBELAJARAN MENDALAM TUMOR PAYUDARA DALAM IMEJ ULTRABUNYI

ABSTRAK

Penggunaan teknik pengimejan ultrasound untuk mendiagnosis kanser payudara pada peringkat awal adalah kaedah yang popular dan berkesan. Isu dengan diagnosis ultrasound payudara tradisional ialah, tidak seperti pengimejan resonans magnetik (MRI) dan mamografi, ia terdedah kepada kesilapan kerana subjektivitinya, yang boleh mengakibatkan diagnosis terlepas dan biopsi yang tidak perlu. Dalam projek penyelidikan ini, algoritma model klasifikasi tumor payudara baru-baru ini disiasat dan dianalisis, dan kemudian batasan dan jurang dalam teknik sebelumnya diserlahkan. Set data Imej Ultrasound Payudara telah disediakan dan diproses terlebih dahulu untuk melatih kedua-dua model pengelas U-Net dan rangkaian neural Convolutional. Model U-Net digunakan untuk mengesan pertumbuhan tumor dalam imej perubatan asal kerana kapasitinya untuk melakukan klasifikasi pada setiap piksel dalam imej input dan menghasilkan imej input dan output yang mempunyai saiz yang sama. Kemudian, model pengelas CNN dibina untuk mengklasifikasikan imej topeng yang dihasilkan oleh model U-Net sebagai jinak, malignan atau normal. Metrik prestasi ketepatan dan fungsi kehilangan Dadu digunakan untuk menilai prestasi kedua-dua model pengelas U-Net dan CNN. Model U-Net telah mencapai ketepatan 93% dan nilai kehilangan dadu sebanyak 0.4391. Manakala model pengelas CNN telah mencapai ketepatan 85%.

ACKNOWLEDGEMENTS

I would also like to express my gratitude to my family for their moral support and warm encouragements. Also, I would like to thank Dr. Ahmed for a grant that made it possible to complete this study. Finally, I would like to express my deepest gratitude to IR. DR. LAI KHIN WEE whose comments and suggestions were innumerably valuable throughout the course of my study.

TABLE OF CONTENTS

LIST OF FIGURES

LIST OF TABLES

LIST OF SYMBOLS AND ABBREVIATIONS

MRI	:	Magnetic resonance imaging
BUID	:	Breast Ultrasound Images Dataset
CNN	:	Convolutional neural network
WHO	:	World Health Organization
CAD	:	Computer Aided Diagnosis
CT	:	Computed tomography
FFDM	:	Full field digital mammography
DM	:	Digital Mammography
DBT	:	Digital breast tomosynthesis
ANN	:	Artificial neural network
WSI	:	Whole-slide imaging
PET	:	Positron emission tomography
ROI	:	Region of interest
HP	:	Histopathologic
DNN	:	Deep neural networks
BCDR	:	Breast Cancer Digital Repository
DDSM	:	Digital Database for Screening Mammography
SVM	:	Support Vector Machine
ML	:	Machine learning
ReLU	:	Rectified linear unit
HEF	:	Hand-engineered features

LIST OF APPENDICES

CHAPTER 1: INTRODUCTION

1.1 Overview

Despite advancements in cancer treatment, cancer is still regarded as a major public health concern worldwide because of its ability to arise almost anywhere in the human body where cells start to multiply uncontrollably. Various factors such as the aging population and the prevalence of certain lifestyle habits have been identified as contributing factors to the cancer rate (Dronkers et al. 2002). Deaths caused by cancer are on the rise globally. In 2015, around 8.8 million people died due to the disease (World Health Organization 2018) and according to the World Cancer Research Fund (2014), there has been a 20% increase in the past decade, and it is estimated that 27 million new cases will occur globally by 2030.

Breast cancer has an extremely high mortality rate when compared to other cancers where it is considered the second most common type among women after skin cancer. According to the International Agency for Research on Cancer, in 2012, breast cancer mortality increased by 14% whereas cancer mortality climbed only by 8% (Ferlay et al. 2013). In addition, the World Health Organization (WHO) stated that breast cancer is considered the main cause of cancer-related deaths among women in Malaysia. In 2018, the organization noted that the mortality rate for breast cancer was 11.0% in Malaysia, which is the highest among the other types of cancer.

Studies have shown that early detection of breast cancer can lead to a reduction in mortality rates by 38% from 1989 to 2014 (Siegel et al. 2017). Currently, biopsy is the gold standard for detecting breast tumors (Qu et al. 2019). However, it is considered an invasive technique that has poor repeatability and can cause bruising and infection (Byra et al. 2016). In addition, less than 30% of the breast tumors detected using a biopsy are malignant (Huang et al. 2019). The use of mammography and ultrasound imaging technology is a popular and successful way for detecting breast cancer early (Akin et al.

2012). However, mammography imaging is commonly unsuitable for women with dense breasts in 20-50% of cases (Eisenbrey et al. 2016). Furthermore, women with glandular breast tissue are significantly more likely of being diagnosed with breast cancer than women that have fatty breast tissue (Piotrzkowska et al. 2016).

Instead of using a traditional procedure, opting for ultrasound imaging can help improve the detection of breast cancer by 17% and also reduce the unnecessary biopsies performed on patients by 40% (Cheng et al. 2010). Ultrasound is a non-ionizing, low-cost, real-time medical imaging modality that is safer, more versatile, and sensitive to tumor cells in dense areas (Stavros et al. 1995). However, the issue with conventional breast ultrasound diagnosis is that it is prone to making a mistake due to its subjectivity, unlike magnetic resonance imaging (MRI) and mammography, which could result in a missed diagnosis and an unnecessary biopsy (Huang et al. 2019). Due to the difficulties and the appearance of speckle noise in ultrasound images, it requires specialist radiologists to explain them properly. As a consequence, Computer Aided Diagnosis (CAD) is used to help radiologists in the classification and diagnosis of breast cancer using ultrasound.

Various studies conducted on ultrasound breast imaging revealed that the use of CAD systems provides strong diagnostic performance and low observer variability (Singh et al. 2011). Feature extraction, selection, and classification are all considered standard CAD procedures where having a good feature extraction technique can help to increase the overall performance (Newell et al. 2010). However, the process of extracting and selecting the relevant image features from the data is very time-consuming and requires a lot of manual work and resources such as pre-processing procedures. In addition, because of the speckle and noise in ultrasound imaging as well as the employment of numerous algorithms, the fine-tuning of traditional CAD systems becomes more challenging. These issues prompted the creation of new techniques, such as deep learning

algorithms, which can automatically learn features and extract non-linear features from the input data. Deep learning techniques are shown to be effective and promising in in terms of pattern recognition and classification of ultrasound images where it is difficult to achieve by hand (Singh et al. 2020). Furthermore, deep learning techniques can extract complex higher-level attributes by layer and learn straight from raw input which allows them to perform better in terms of pattern recognition and segmentation.

1.2 Problem Statement

The use of mammography and ultrasound imaging techniques to detect breast cancer early is considered a popular and efficient approach. However, because breast density has no effect on ultrasound waves in the breast, ultrasound imaging is considered a safe and effective procedure for women. The problem with conventional breast ultrasound diagnosis is that, unlike magnetic resonance imaging (MRI) and mammography, it is prone to making a mistake due to its subjectivity, which could lead to a missed diagnosis and an unnecessary biopsy. In ultrasound imaging, the radiologist's skill is essential for feature extraction, which is a challenging and time-consuming task that requires multiple pre-processing procedures and is often dependent on human work, resulting in subject diagnosis. Furthermore, due of speckle and noise in ultrasound imaging, as well as the use of multiple algorithms, fine-tuning conventional CAD systems becomes more difficult, necessitating the need of specialized radiologists to correctly explain them.

1.3 Objectives

1. To conduct a critical analysis and comparative study on the existing and recent algorithms of Breast tumors classification systems.
2. To propose a deep learning image classification model that classifies breast tumors into benign, malignant, or normal.
3. To evaluate and measure the accuracy of the proposed model.

1.4 Methodology

Initially, the existing and recent algorithms of breast tumor classification models are investigated and analyzed, then the problems and gaps existed in previous approaches are identified. Next, the Breast Ultrasound Images Dataset is prepared and preprocessed in order to train both U-Net and the CNN classifier models. The U-Net model is used in this project to localize areas that contains tumor growth in the original medical images, because of it is ability to perform classification on each pixel in the input image, producing input and output images that are the same size. Then, a CNN classifier model is constructed in order to classify the generated mask images from the U-Net model into benign, malignant or normal. The network architectures of both U-Net and CNN classifier model are explained in detail in Chapter 3. Lastly, the performance of both U-Net and CNN classifier models is evaluated by using Dice loss function and accuracy performance matrices. Figure 1.1 shows the flowchart of this research project approach.

1.5 Report Organization

The body of this research project is composed of five chapters and one appendix.

The current chapter reviews the background information, all main issues related to breast tumor classification, and provides an overview on the problem statement, objectives, and the methodology of this research project.

In chapter 2, a critical review on related works to breast tumor classification in ultrasound images is presented. The analysis, research papers and studies on the existing techniques are discussed by comparing the strength, weaknesses, and performance of each study.

Chapter 3 presents the methodology of this research project. The collection of the dataset, the network architecture of both U-Net and CNN classifier models are discussed in this chapter.

In chapter 4, the dataset preparation and the implementation details are presented as well as the results and evaluation of the proposed U-Net and CNN classifier models.

The summary of this research project is presented in chapter 5 as well as the future work where the extension of the current approaches and evaluations are discussed.

Lastly, Appendix A shows the source code used for classifying breast tumors in ultrasound images.

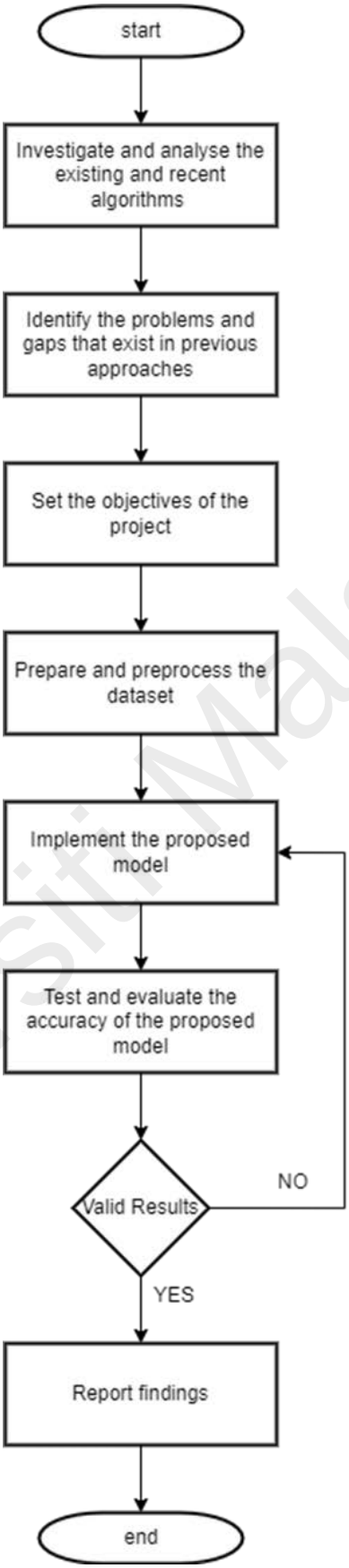

Figure 1.1: Flowchart of the research project approach

CHAPTER 2: LITERATURE REVIEW

2.1 Overview

In an effort to automate the diagnosis of breast lesions and reduce the need on operators in ultrasound imaging, various algorithms including CAD tools were used by researchers to classify and localize the lesions. The results of these research revealed that the CAD systems used for the classification and localization of the lesions performed well where it had a strong diagnostic performance and low observer variability. Deep learning approaches have recently gained a lot of attention due to their ability to interpret large data sets and their high discriminability power. These techniques including deep CNNs have improved performance significantly and been widely used in image classification and object detection. Although there are various approaches that have been developed to automatically classify breast lesions, most of these involve small datasets and require additional evaluation. In addition, some of these methods rely on the texture features extracted from a single image, which is usually speckled and has low contrast. These factors can affect the performance of the proposed texture methods. In order to provide a broad overview of breast ultrasound image classification, this chapter reviews recent breast ultrasound image classification approaches as well as potential difficulties that may arise during the classification process. In addition, the available gaps in related studies are reviewed in this chapter.

2.2 Medical Imaging Modalities

Medical imaging modalities are used more commonly and are considered to be more efficient than other testing techniques for the detection of breast cancer. Mammography, MRI, ultrasound imaging, computed tomography (CT), and histopathology images are common medical imaging modalities that applied for diagnosing breast cancer.

2.2.1 Mammogram

Mammograms allow radiologists to detect for abnormalities in the breast tissues. Mammograms have already been researched over the past 20 years and are generally recommended in the early stages of breast cancer, referred to as Mammogram screening which can be seen in Figure 2.1a. A radiologist examines a mammography for the existence of a mass (lump or cyst), as seen in Figure 2.2, as well as small calcium deposits known as micro-calcifications, which appears as tiny flecks or white spots as shown in Figure 2.1b.

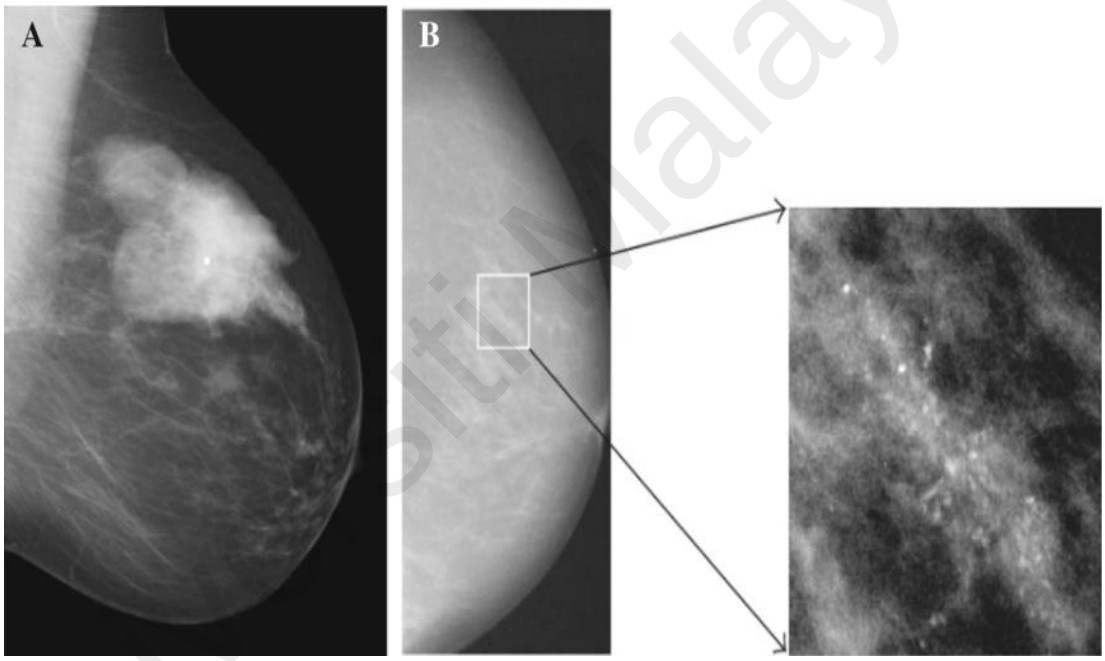

Figure 2.1: a) Masses with variable densities reflecting the presence of soft-tissue density and fat elements. b) On the left is a mammography image; on the right is a magnified view of clustered microcalcifications (James et al. 2016).

Due to the advancements in medical imaging technology, breast examinations have been categorized into three categories: screen film mammography (SFM), digital breast tomosynthesis (DBT), and full field digital mammography (FFDM). digital mammography (DMs) and SFMs are considered two-dimensional grayscale images,

whereas DBT gives several frames of two-dimensional grayscale image sequences that looks like black-and-white video.

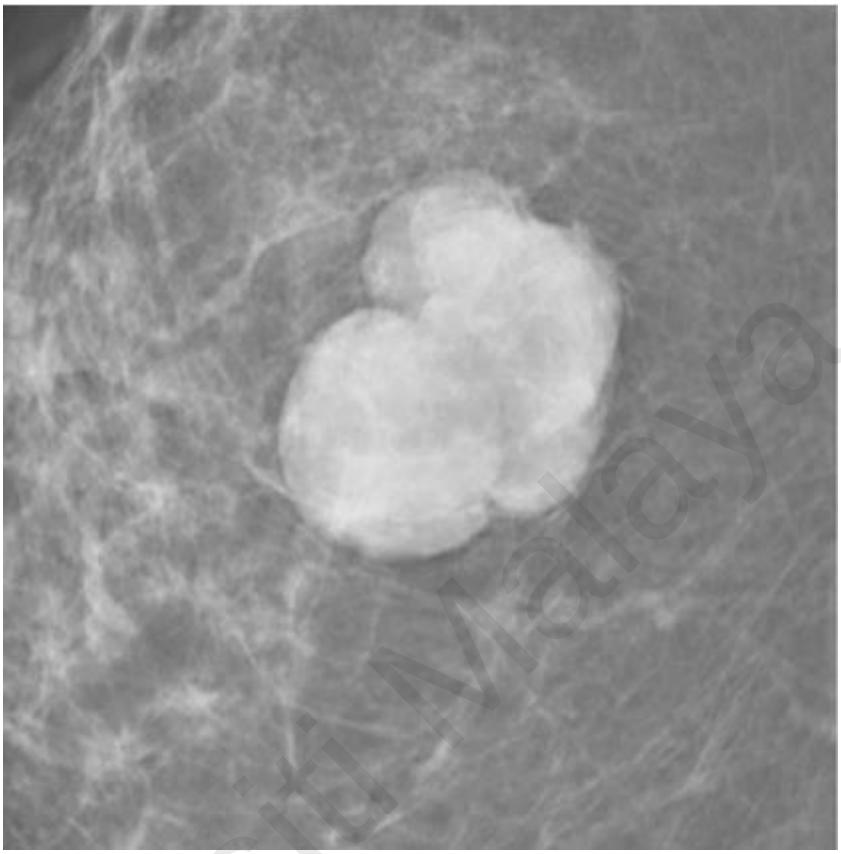

Figure 2.2: Mammogram with well-defined rounded mass

In many studies, the traditional SFM images have been used to classify breast cancer. For instance, Dhungel et al. (2017) developed an integrated model that could detect and classify breast cancer into malignant or benign masses utilizing SFM. Likewise, Emperumal and Duraisamy (2017) presented a unique approach that combines the features of the traditional SFM images with the Chan-Vese level set method to classify breast cancer into different types.

The second category of digital mammograms, known as DM, is commonly used for breast cancer classification by numerous researchers. Carneiro et al. (2017) proposed a

comprehensive method in order to classify unregistered digital mammograms into benign, malignant, and normal lesions. In addition, Qiu et al. (2017) have presented an approach that could classify tumors by using DM without feature selection, feature extraction, or lesion segmentation. As for the third category, 3D mammography, or DBT, is considered the most sophisticated mammography technique used. This technology takes multiple images and combines them into a single video. However, because of the limited number of available image datasets, only few studies are conducted by using DBT for breast cancer classification. Kim et al. (2016) presented a model that can classify breast cancer by discovering the latent bilateral representations of tumors using volume of interest in DBT.

A follow-up study conducted by Samala et al. (2018) proposed an effective model that can perform binary classification of breast cancer using various types of digital mammograms including DBT, FFDM, and SFM, by minimizing the number of computations. Most studies on image classification rely on either SFM or DM. SFM is more commonly used due to its ability to produce images directly on large sheets of film. Moreover, compared to other imaging technologies, such as DBT and FFDM, SFM is more cost-effective and easier to use. FFDM images, on the other hand, are much easier to store, print, view, and edit on a computer. As a result, because of the processing power of digital images, they are viewable on a computer screen with various features such as zooming and contrast enhancement. Therefore, the majority of current public datasets used by academics are digital mammograms rather than SFMs because of the processing efficiency in digital images (Murtaza et al. 2020).

Nevertheless, researchers began to employ DBT for a variety of reasons. For example, as compared to FM or DM, DBT could provide a clear picture of the breast from many angles, allowing for a more confident diagnosis and reducing the need for follow-up

examination (Radiological Society of North America 2018). In addition, DBT is capable of reducing the false negative in mammograms because of its ability to analyze a vast number of pictures in video form for each subject. Despite the popularity of mammography diagnosis, certain cases could have dense breast tissue or thick skin, making the malignant area nearly unnoticeable. This issue can increase the false negative rate and cause the cancer to remain undetected. When image analysis is suspicious, it is usually suggested that a comprehensive evaluation be conducted, which includes various tests such as MRI, CT, and positron emission tomography (PET).

2.2.2 Magnetic Resonance Imaging

Magnetic resonance imaging (MRI) is a type of imaging that uses radio waves and magnetic fields to visualize the soft tissues of the body, such as liver, lung, or breast as seen in Figure 2.3. Thus, breast MRI can provide clear images of the breast compared to other medical imaging methods such as ultrasound, CT, or mammograms images (Tessa and Keith 2018).

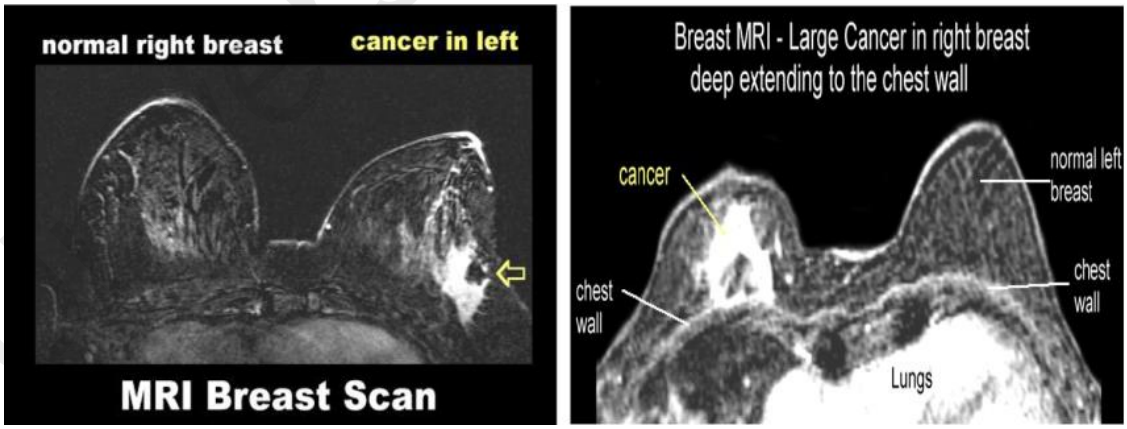

Figure 2.3: Breast MRI image samples

In addition, MRI can help identify areas of concern during a breast biopsy which can be used for MRI-guided biopsy of the breast. MRI machine works by capturing several

breast images of one subject and then combined into a thorough representation. Therefore, it can provide detailed information about the disease, and it is generally requested after the cancer is diagnosed (MFMER 2018). Unfortunately, few studies are conducted on the use of MRI to classify breast cancer (Bevilacqua et al. 2016; Amit et al. 2017; Rasti et al. 2017) due to the lack of accessible datasets.

Moreover, Bevilacqua et al. (2016) used an Artificial neural network (ANN) to identify benign and malignant breast cancer by extracting and using features from MRI images. On the other hand, in a study conducted by Amit et al. (2017), they used CNN to classify the breast MRI images into various classes after extracting regions of interest (ROI) from the images. They also injected a contrast agent into the body before dynamic contrast enhanced MRI (DCE-MRI) in order to improve the quality of the images. This method can yield colorful parametric views as well as grayscale images with improved contrast to give specific details about malignant tissues (Moon et al. 2009). Nevertheless, only one research was able to benefit from DCE-MRI for the classification of breast cancer. In this study, Rasti et al. (2017) utilized an exclusive dataset in order to train a CNN framework that classifies the breast tumor using DCE-MRI images.

2.2.3 Histopathologic Images

Histopathologic (HP) biopsy imaging is performed using a microscope by collecting and analyzing tissue samples from a region of the breast. The specimens are stained using hematoxylin-eosin, which is a substance commonly used in medical procedures in order to examine for malignant tissues. Later, the stained slides are digitized and transformed into WSIs, which are digitally colored images as shown in Figure 2.4. Most of the time, expert pathologists use whole-slide imaging (WSI) to extract region of interest patches by using different zooming factors to diagnose different types of cancer, such as breast cancer and non-invasive cancer as shown in Figure 2.5.

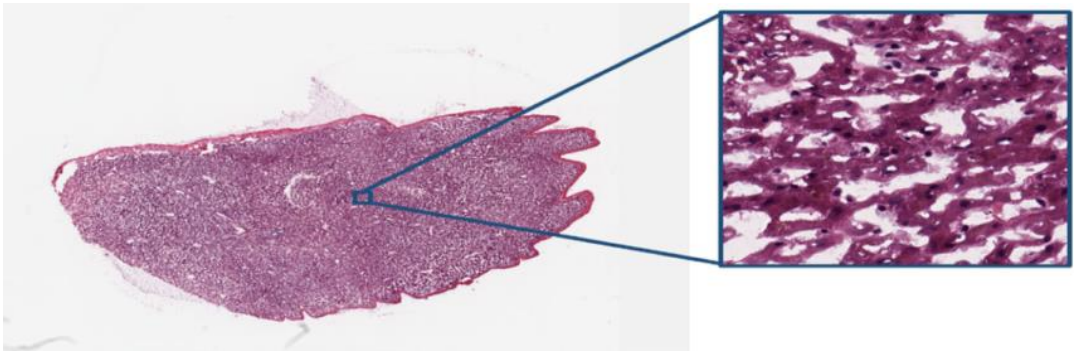

Figure 2.4: Histopathology WSI is presented at low magnification on the left, whereas the right side displays the cropped section at high magnification (Liu et al. 2017)

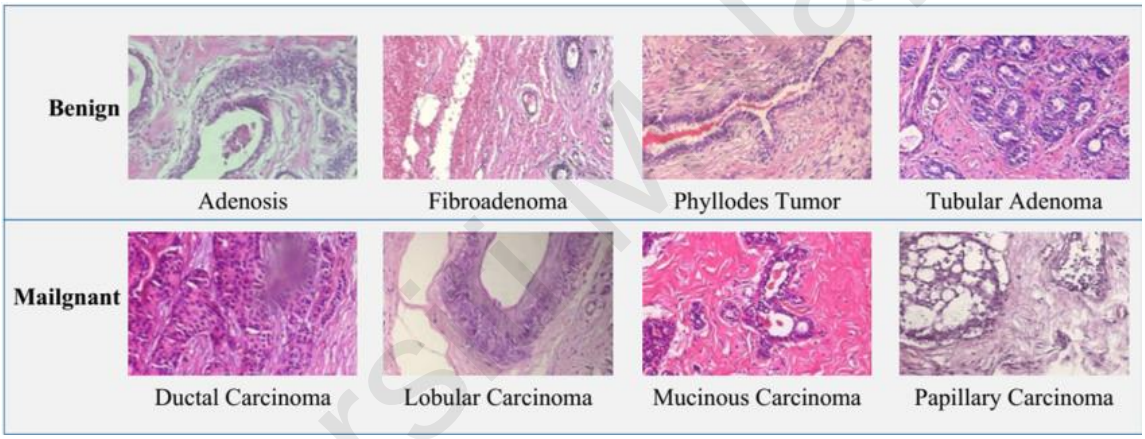

Figure 2.5: Patches of histopathology image displaying eight kinds of breast cancer

With the exception of breast cancer detection, biopsy imaging is considered the gold standard for several forms of malignancies, such as liver cancer, and lung, thanks to tissue level image analysis (Rubin et al. 2008). Many studies have shown that using HP images can help accurately classify breast cancer into multiple classes. For example, Han et al. (2017) employed the images in order to classify the cancer into eight categories. Araujo et al. (2017) conducted another study revealed that using HP images with the developed model can help classify breast cancer into four different types. According to the studies

cited above, using HP images could help with particular subtypes of malignant or benign breast cancer. Compared to mammograms and other imaging modalities, HP images offer several advantages. For example, they can automatically classify breast cancer into many classes rather than binary classes because WSI imagery allows to create a lot of ROI images that needed for training deep neural networks (DNN) models, which can be utilized for monitoring treatment effects and reporting on the status of the disease.

In addition, these images could be uploaded online to receive an expert pathologist's opinion from afar and therefore establish an accurate diagnosis. However, despite the advantages of HP images, they can still be problematic for automatic image classification due to the nature of the procedure involved (Murtaza et al. 2020). Furthermore, creating digital images from gathered biopsy samples takes a long time, and distinguishing between breast cancer subtypes necessitates a high level of competence. In addition, color variation is substantial in the production of HP images due to the various steps involved in the development of these images such as lab protocols, and staining process making it difficult to train a multi-class DNN model quickly, mainly when employing borderline situations.

2.2.4 Ultrasound

An ultrasound image (sonogram) is a type of imaging test which uses high-frequency sound waves to visualize the internal organs of a patient as seen in Figure 2.6. Unlike MRI and mammograms, ultrasound does not involve radiation exposure. Ultrasound imaging can also help diagnose various conditions such as pain and swelling in the body. In addition, ultrasound can be used to assist with breast needle biopsy for the analysis of breast tissues. Ultrasound imaging is not used as a standalone test for breast screening. Instead, it can be utilized to find abnormalities in the breast that are not cancerous where

it could be in the form of fluid-filled regions (cysts) or solid lump (mass) (Murtaza et al. 2020).

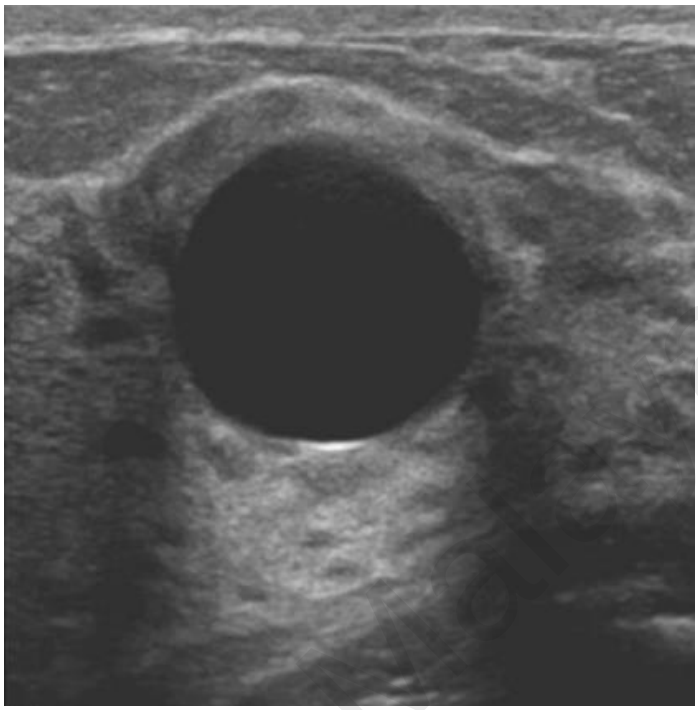

Figure 2.6: Identification of a lump, mass, or cyst by the absence of internal echoes and the posterior enhancement of the ultrasound beam (James et al. 2016)

However, ultrasound has difficulties in telling the difference between a malignant tumor and calcifications. Breast ultrasound, according to some studies, is a preferable choice for diagnosing breast cancer in young women that have fat, bulky, or thick breast skin, especially when a mammogram is unable to properly identify breast cancer tumors. Cheng et al. (2016) designed a method that automatically extracts different features from ultrasound breast images in order to accurately classify malignant and benign breast lesions. Nascimento et al. (2016), on the other hand, extracted and fed hand-engineered morphological features of breast ultrasound images into an ANN system for binary classification of breast cancer. Furthermore, as a result of improved imaging methods, the

ultrasound was equipped with various advanced features, such as Nakagami images as shown in Figure 2.8, and shear-wave elastography (SWE) as shown in Figure 2.7.

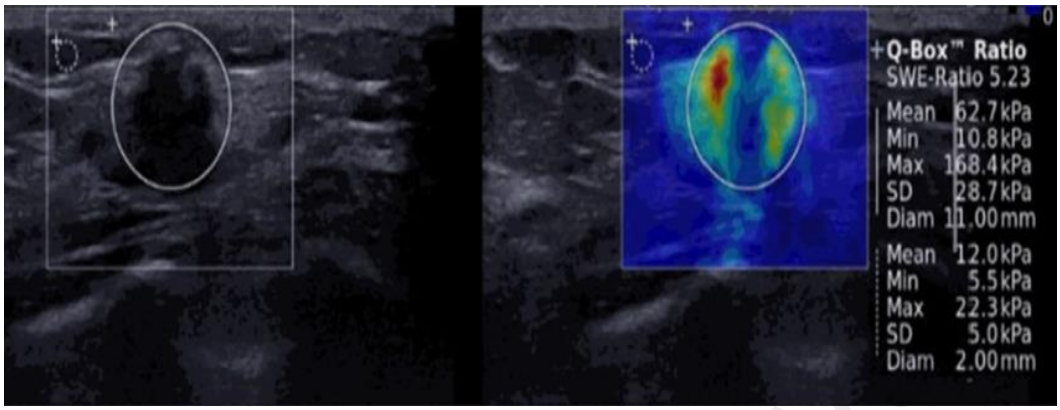

Figure 2.7: Ultrasound image on the left (B-Mode). Heterogeneous elasticity is represented by the irregular red mass in the shear-wave elastography image on the right. Calculations are made to determine the statistical parameters of ROI, such as mean, maximum, and minimum (Youk et al. 2017).

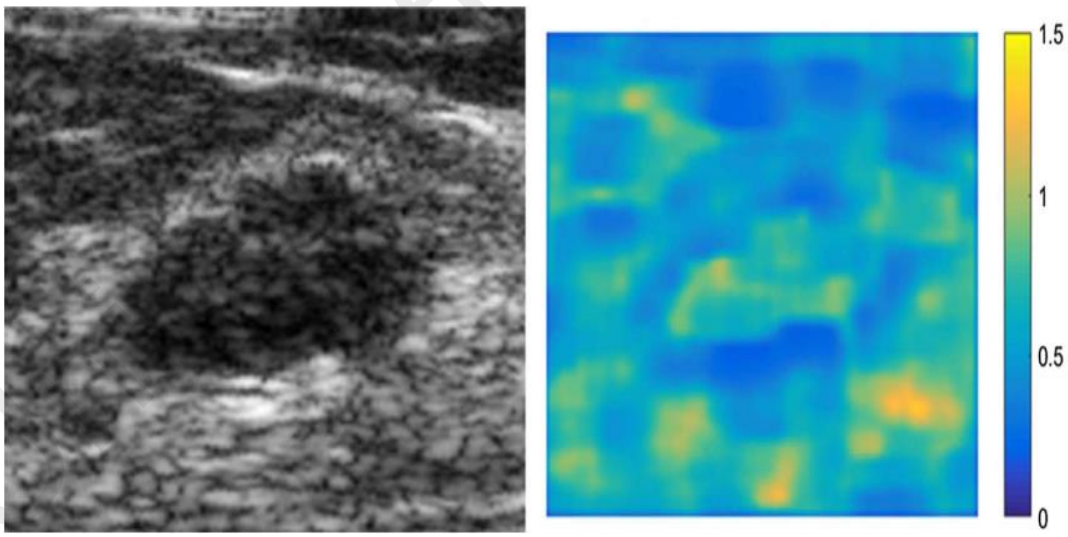

Figure 2.8: Lesion reconstruction in the US image (B-mode) on the left and corresponding Nakagami map on the right

These new features were able to improve the performance of the system. For example, Elastography, recently developed ultrasound method, is commonly utilized to measure

and visualize the tissue elasticity of various organs such as the liver and breast and can also distinguish between malignant and benign tumors (Youk et al. 2017). It is a helpful metric for ultrasound, and it's used to measure tumor grade with a consistent color scheme. As a result, Zhang et al. (2016) utilized SWE images in order to learn features that can help accurately classify breast cancer (malignant or benign) with the help of a deep belief network. Furthermore, for breast cancer analysis, ultrasound images are combined with Nakagami images.

In addition, by combining Nakagami distribution with Nakagami parametric ultrasound images, Tsui et al. (2016) represented tissue characteristics by modelling echo amplitude distribution. Radiologists can use theses color-coded ultrasound images to measure the tissues' stiffness or hardness. As a result, Nakagami and SWE features help to improve the classification of breast cancer. Although the use of Nakagami and SWE techniques has been studied extensively, very few studies have used them to improve breast cancer classification. Byra et al. (2017) presented a model that utilizes CNN to perform a classification of breast cancer by extracting the scattering characteristics breast tissues that been taken from parametric maps of Nakagami images.

However, the new ultrasound technology was only used in a few research. Byra et al. (2017) used a CNN to create a model and extract the scattering features of breast tissues using parametric maps of Nakagami images in order to perform breast cancer classification. One of the causes for the limited publications could be data collection, specifically the difficulties of gathering a big number of medical photos from each medical institution.

2.3 Datasets for Breast Cancer Classification

In order to evaluate the effectiveness of different breast cancer classification models, it is necessary to have a well-defined dataset. The Wisconsin Breast Cancer Dataset

(WBCD), the Digital Database for Screening Mammography (DDSM), the Mammography Image Analysis Society (MIAS), and the Breast Cancer Digital Repository (BCDR) are all public databases for breast cancer diagnosis. As deep learning is getting popular for its ability to handle images in hierarchical form using nonlinear transformations, researchers frequently use ultrasound images in their work. (Rezaeilouyeh et al. 2016).

In general, exclusive datasets have fewer annotated images than public datasets. As a result, by evaluating the efficiency of established classification models, experts can develop breast cancer classification techniques. As a consequence, the models that has been evaluated on public datasets are considered more dependable than the models that has been evaluated on exclusive datasets. However, on the level of abstraction, grayscale images such as ultrasound, MRI, and mammogram or colored images such as HP images are applied for breast cancer classification, regardless of the database type whether it is public or exclusive.

The analysis of datasets shows that most previous studies employed mammogram datasets and focused on either binary or tertiary breast cancer classification. BCDR, DDSM, and Breast Cancer Histopathological Database (BreakHis) are considered the most commonly used and authenticated datasets in ultrasound, mammogram, and HP imaging modalities, respectively, since they include a significant amount of data of many subjects, which are essential for training deep neural network classification models with accuracy and confidence. Contrary to popular belief, there are no public datasets that been used for MRI, PET, or CT modalities maybe because of the lack of accessible datasets which is a big factor, or the public datasets did not contain sufficient images to train a breast cancer classification model that based in DNN. Table 2.1 shows an overview of some publicly available datasets used to classify breast tumors.

Table 2.1: Review of publicly available datasets used for breast cancer classification

Imaging modality	Dataset name	# Patients	# Images	Class labels	Study
Mammograms	BCDR-F03	344	736	Benign, Malignant	Duraisamy and Emperumal (2017)
	DDSM	2620	10480	Benign, Malignant	Kumar et al. (2017)
	INBreast	115	419	Normal, Benign, Malignant	Kumar et al. (2017)
	MIAS	161	322	Benign, Malignant	Duraisamy and Emperumal (2017)
Mammograms and Ultrasound images	BCDR	1010	3703	Benign, Malignant	Bakkouri and Afdel (2017)
Histopathology Images	BreakHis	82	7909	Benign, Malignant	Bardou et al. (2018)

2.4 Breast Cancer Image Classification using Deep Learning

Previously, conventional machine learning approaches such like Naive Bayes (Kharya et al. 2014), Support Vector Machine (SVM) (Asri et al. 2016), and Random Forest (Octaviani et al. 2018) were used to classify breast cancer images. Machine learning entails designing and implementation of algorithms that evaluate data and associated attributes in the absence of any previous task which is based on specified inputs out from the environment (Komura et al. 2018). Conventional machine learning approaches focus on feature extraction quality, which is limited to several problems due to the shallow classifier (Rezaeilouyeh et al. 2016).

Deep learning algorithms have recently been shown to produce more encouraging results, particularly on huge and complicated datasets (LeCun et al. 2015). DNNs are a machine learning (ML) technique and AI approach that allows automatic feature extraction used in deep learning. Generally, if more than one hidden layer is used between

the output and input layers of a neural network (NN), the term "deep" is used (Svozil et al. 1997). Unlike conventional ML algorithms, that use hand-engineered features (HEFs) in order to provide optimal results, DNNs utilize representation learning in order to automatically identify complicated feature representation. DNN's mathematical formulas are the main key for its empirical success (Goceri 2018).

DNNs have mostly been employed for face recognition (Parkhi et al. 2015), speech recognition (Amodei et al. 2016), medical image diagnosis, and natural language processing over the years (Lakhani and Sundaram 2017). The capabilities of deep learning to extract important features from unprocessed breast cancer images without depending on generated HEF has driven the growth of deep learning research. In comparison to machine learning that has hand-crafted features, feature learning techniques in deep learning allows to cut computing time while still achieving considerable accuracy (Wang et al. 2014). Due to the automatic learning feature which has been established in order to directly assess the complexity and diversity of images, deep learning surpassed the conventional technique in CAD systems. As a result, the CNN is considered the most popular model being used for diagnosis of breast cancer (Fujita, 2019).

Modern computational power has the ability to help solving the related challenges and the enhancement of community health and quality of life. Deep learning is considered a well-known and still-developing technique among machine learning researchers. The major goal of using deep learning in image identification and is to find several levels of representations based on learning algorithms that are focused on higher-level features (LeCun et al. 2015). It is primarily concerned with learning algorithms that can develop, learn, and improve on their own in order to process data. Internal representation can be extracted using deep learning methods from high-dimensional images (Kiambe et al. 2018).

Conventional Machine learning performs effectively with structured data that has lots of characteristics or features. However, the analysis procedure for unstructured data will become complicated, if not impossible. Unstructured data, such as text data, images, media, and audio, are stored in an unstructured format that is not dictated by data models. Deep learning uses a model architecture made up of several non-linear variations and processing layers to model distinct fundamental or desired features in data (LeCun et al. 2015)].

Deep learning has recently gotten a lot of interest from researchers because of its success in handling challenges with unstructured data. Deep learning can help radiologists make an early diagnosis of breast cancer using ultrasound images in the medical field. Deep learning methods have recently successfully helped in image analysis, signal processing, and breast cancer classification (Khairi et al. 2021).

The CNN is a type of deep learning model which could be used to accurately classify images and extract features. Zuluaga-Gomez et al. (2021) developed a CNN-based deep learning architecture in 2021 to visually recognize and detect patterns using the thermal images from DMR-IR database. The researchers developed Tree Parzen Estimator (TPE), a Bayesian optimization, as the hyper-parameter for optimizing the algorithm. The CNN technique demonstrated a competitive improvement of 92% accuracy in experimental results. The research also showed that data augmentation and data pre-processing can improve model performance. Moreover, Alom et al. (2019) presented a unique CNN model for multi-classification of breast cancer with various data augmentation strategies that relies on inception and residual networks. When compared to models which have been built on data-driven and learning for multi-classification, the studies revealed an increase in accuracy of about 0.55% (Patient-level) and 1.05 %(image-level).

Hijab et al. (2019) used Transfer Learning to fine-tune the VGG16 network and to diagnose breast cancers using a database of 1300 ultrasound images. In addition, to avoid overfitting, image augmentation has been employed by the author to enlarge the dataset and create a new one with 21,600 photos, which was divided into 15120 images used for training and 6480 images used for testing. Then, the updated training set has been utilized to fine-tune the weights on the VGG16 network's final convolutional layer and assess the system's performance in classifying the images in the testing set. The researchers attained accuracy and AUC values of 0.97 and 0.98, respectively. Although the findings were excellent, only a small percentage of the dataset was tested, and some image augmentation methods, like shearing, are not advised for these types of images (Zhou et al. 2017).

The authors of (Byra et al. 2019) employed transfer learning in order to adjust and train a well-known CNN network for breast tumor classification using ultrasound images. A total of 882 images were used in their research where they created a training and testing set from the dataset. Furthermore, the grayscale images pixel intensities were rescaled and converted to three independent RGB channels using a matching layer throughout the training stage. After some fine-tuning, the VGG19 network has been adapted for training where an AUC value of 0.936 was obtained. The authors claim that this performance outperformed radiologist readings in terms of classification accuracy.

The authors of (Wang et al. 2020) employed transfer learning in order to adapt an Inception-v3 CNN, which is considered GoogLeNet's 3rd generation, for classification of breast tumor using ultrasound images. 316 breast lesions were used to train and assess the proposed CNN (181 benign and 135 malignant). With five-folder cross validation, the presented CNN obtained an AUC of 0.9468, whereas the sensitivity and specificity were found to be 0.886 and 0.876, respectively.

Despite the fact that CNNs are quite good at automatically extracting features and classifying objects, the authors of (Sakr et al. 2019) argue that they cannot generalize well because there is not enough labelled data. As previously stated, only few publicly available labeled databases of breast lesions on ultrasound images are available. As a result, most of studies only used a small number of labelled data to train the network. In some of these studies, the sensitivity and AUC value obtained were insufficient for clinical usage, while in other studies, there is no reason for utilizing a deep neural network for image classification with a limited dataset.

CHAPTER 3: METHODOLOGY

3.1 Overview

The use of a variety of methodologies and methods have been highlighted in this chapter to meet the pre-processing goals for the Breast Ultrasound Images Dataset (BUID) in order to train and test the proposed model where various pre-processing methods for the BUID been investigated.

Cropping the original images, manually examining the images, and resizing the images have all been explored as techniques of processing the image input size. Next, the U-Net model is employed in this study to locate tumor growth in the original medical images since it can classify each pixel in the input image, which results in input and output images of the same size. The generated mask images from the U-Net model are then classified as benign, malignant, or normal using a CNN classifier model. In this chapter, a thorough explanation of the network architectures of the U-Net and CNN classifier models is presented where both models hyperparameters such as momentum and learning rate are examined to determine the project's baseline parameters.

In addition, the neural network layers of the CNN are fine-tuned and optimized. Finally, the accuracy and loss for each epoch trained are measured, and the best results for each model are used. Figure 3.1 illustrates the overall framework of this research project. Physical materials are not used for the proposed deep learning model. Instead, Python has been selected as the programming language and associated libraries.

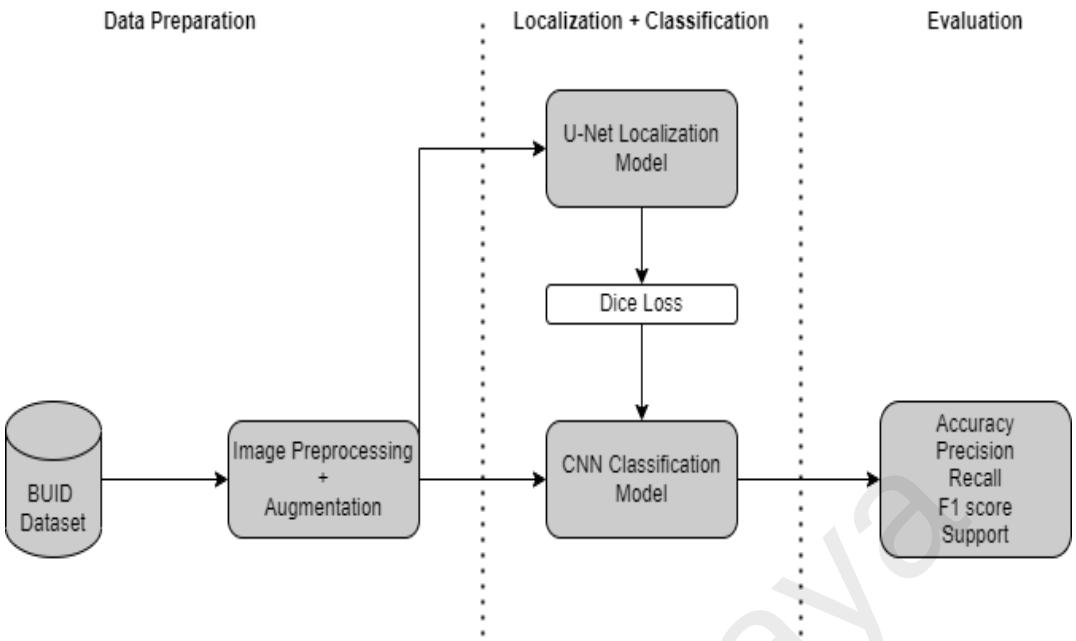

Figure 3.1: The proposed framework of this research project

3.2 Dataset Description

One of the main elements to develop an effective model for detecting and classifying breast tumor is to collect and process a sufficient number of breast ultrasound images. Therefore, in this project the BUID (Al-Dhabyani et al. 2020) is used which is available publicly. The BUID contains 780 greyscale images in the format of PNG with an average image size of 500 x 500 pixels. Al-Dhabyani et al. (2020) have collected Breast ultrasound images from 600 female patients aged 25 to 75 years old for their project in 2018. The dataset is divided into three classes: malignant (210 images), benign (437 images), and normal (133 images), with each image having its own mask image and the ground truth images are presented with original images. Samples of the dataset are shown in Figure 3.2.

Figure 3.2:Normal, malignant, and benign lesion samples in BUID dataset

3.3 Image Pre-processing

In order to perform the classification process, the Breast Ultrasound Images Dataset must be preprocessed before they can be used. Preprocessing is the process of modifying images so that they can be used in the model. Because the model does not recognize images of variable sizes, preprocessing is required to ensure that all the images are of the same size. The images must be of the same dimensions. There are numerous

techniques to alter the images in this way so that the model can interpret them easier and produce better results.

3.3.1 Image Resizing

The most critical stage in pre-processing is modifying the dataset in a way that keeps the original content of each image as much as possible while keeping the entire dataset consistent in terms of image size. This could involve resizing to maintain the original aspect ratio, cropping to focus on critical sections of the image, or modifying the color dimensions of each datapoint, such as contrast, brightness, and more. Cropping is the method of reducing the size of an image to a smaller size. This usually entails removing a portion of a border in order to reduce the size. Zero-padding is the inverse of cropping, in which a border is added to the image, usually black, to make it larger. Both of these methods are the simplest ways to ensure that all images are the same size. Cropping, on the other hand, may remove essential elements from the image, causing the model to provide an incorrect answer, whereas zero padding may throw the model off because of the unwanted black border around images. In well-known and recent CNN architectures, grid sizes of 128x128, 224x224, or 320x320 pixels are the most prevalent options (Pal et al. 2016). In this project, all the images were resampled to 128 x 128 pixels as seen in Figure 3.3. In addition, to train the U-Net model the dataset is split into 95% for training and 5% for testing, whereas for the CNN classifier the dataset is split into 90% for training and 10% for testing.

3.3.2 Normalization

In image processing, normalization is used to adjust the intensity level of pixels. It is used to improve the contrast of images that have low contrast because of glare. In this project, image normalization was performed on all of the images in the datasets to produce

a constant dynamic range, where the dataset has been divided by 255 because of the fact that it contains gray scale images as seen in Figure 3.4.

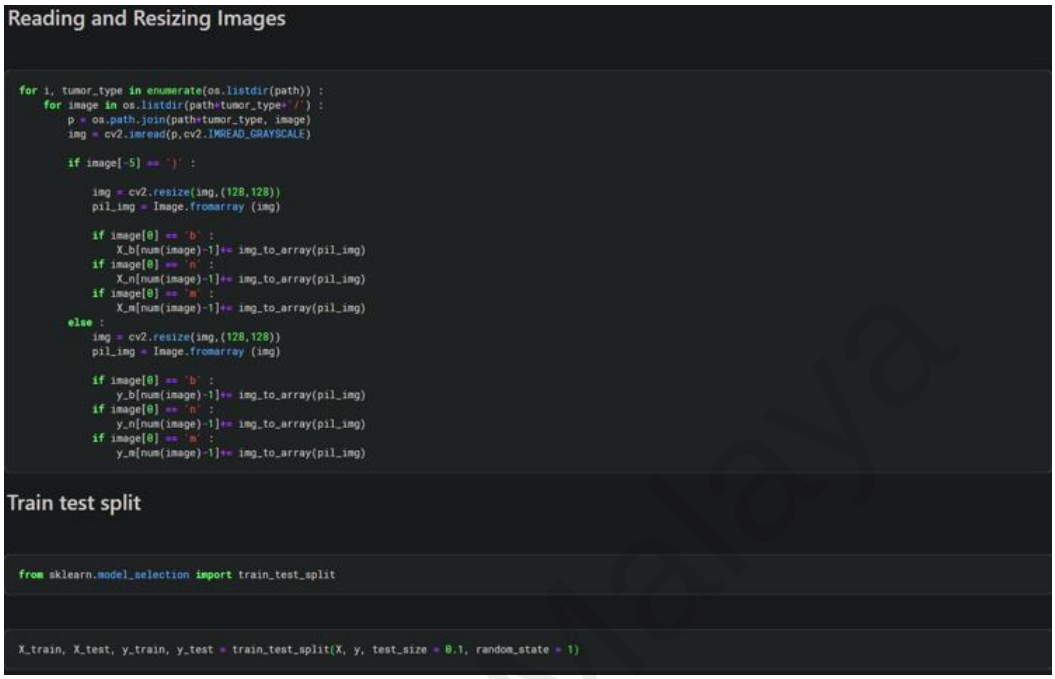

Figure 3.3: The process of resizing and splitting the images into training and testing sets

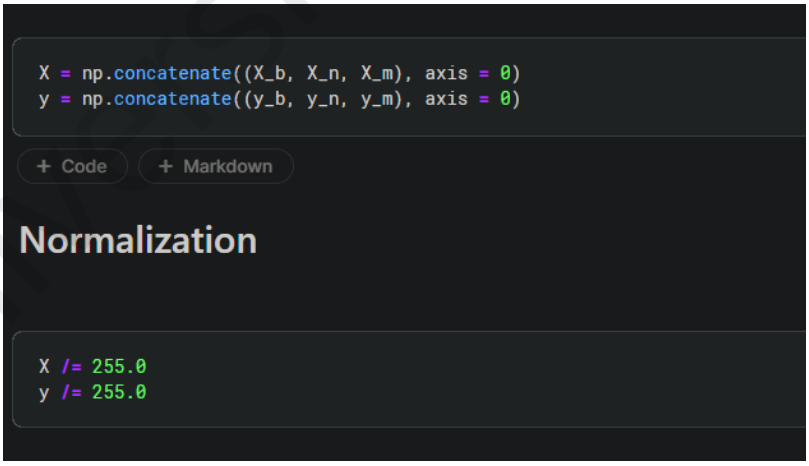

Figure 3.4: Applying normalization to the dataset

3.3.3 Data Augmentation

Whenever a small number of datasets is used to train the model, transformation of the training images is essential. Data augmentation is one of the methods used in order to

transform the images. Image data augmentation is a technique for artificially increasing the size of a training dataset by modifying images in the dataset. Because the dataset only contains limited images, data augmentation prevents a neural network from learning irrelevant features which leads to improved model performance. Cropping, horizontal flipping, color shifting, rotation, and other techniques can be used to modify the training data. The augmentation techniques used in this research is to randomly flip the training images horizontally to modify the input images. In this project a function a function is defined to do simple augmentation techniques such as rotation, flipping, zooming, and so forth as shown in Figure 3.5. As a result of transforming the images, more new and diverse training samples are created, which improves the training results.

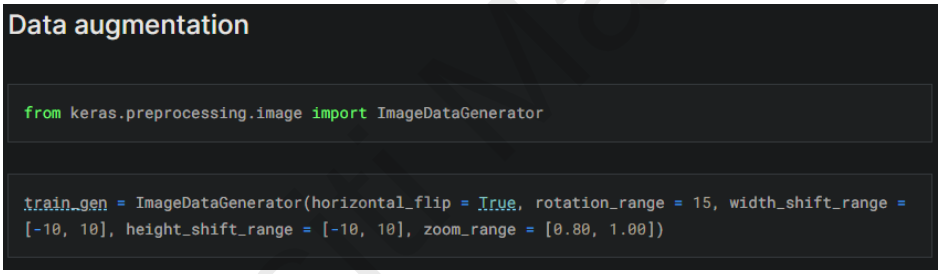

Figure 3.5: Applying data augmentation techniques to the dataset

3.4 U-Net Architecture

In 2015, U-Net, which evolved from the standard CNN, was designed, and used to process biomedical images for the first time (Ronneberger et al. 2015). Convolutional networks are frequently employed for classification tasks in where the output is usually a single class label. However, localization should be part of the desired output in many visual tasks, particularly in biomedical image processing, where each pixel has to be given a class name. U-Net is committed to resolving this issue. It has the ability to localize and discern borders since it performs classification on each pixel in the input image, resulting in the input and output having the same size.

As illustrated in Figure 3.6, the U-Net is made up of both an expansive path (shown on the right) and a contracting path (shown on the left). The convolutional network's contracting path has the conventional architecture of convolutional network. It made up of two 3 x 3 convolutions which are applied repeatedly, each one followed by one rectified linear unit (ReLU) and 2 x 2 max pooling operation that has stride 2 used for down sampling. In addition, the feature channels numbers are doubled with each down sampling step.

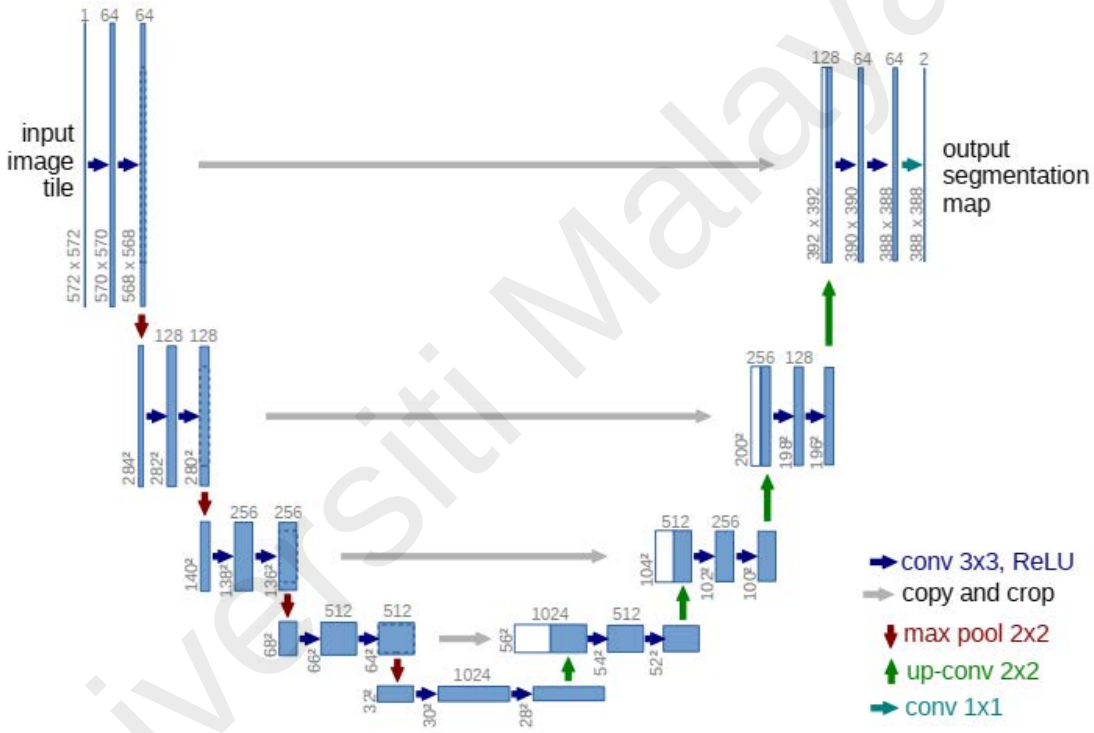

Figure 3.6: U-Net architecture (Ronneberger et al. 2015)

Each stage in the expansive path begins with an upsampling of the feature map, then it is followed by a 2x2 convolution layer which cuts the feature channels numbers in half, then a concatenation with the correspondingly cropped feature map from the contracting path, and lastly, two 3 x 3 convolutions layers where each layer reinforced by a ReLU. Because of the loss of border pixels throughout all convolution layers, cropping is

considered an important process. A 1x1 convolution has been applied at the final layer in order to map each 64-component feature vector to the appropriate number of classes. To ensure that the output segmentation map tiles seamlessly as shown in Figure 3.7, the input tile size should be chosen so that all 2x2 max-pooling actions are performed to a layer with an even x- and y-size. The empty context is extrapolated through mirroring the input image in order to predict the pixels within border region of the image. Since the GPU memory would otherwise be a constraint on the resolution, this tiling technique is essential for using the network on large images (Ronneberger et al. 2015).

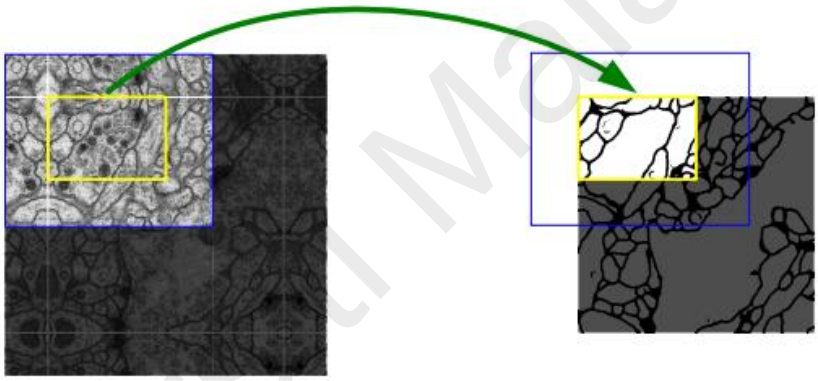

Figure 3.7: Overlap-tile segmentation strategy for arbitrary large photos. Image data from the blue area is required for segmentation prediction in the yellow area.

In the project, small modifications are made to the U-Net architecture. The padding is kept the same in order to obtain a mask with the exact same dimensions as the original image. In addition, the Adam gradient descent method was applied, with a learning rate of 0.00005. Furthermore, the BatchNormalization, which was found after U-net, is introduced in order to normalize the contributions to a layer for each mini-batch, which has the effect of settling the learning process and substantially reducing the number of training epochs needed to train deep neural networks.

3.4.1 Loss Function

The loss function calculates the difference between the algorithm's current output and its predicted output. This is a technique for assessing how well the algorithm fits the data. The Dice loss function is employed in the project to evaluate how well the U-Net prediction model predicts the expected result. In the field of computer vision, the Dice coefficient is a popular statistic for determining how similar two images are (Carole et al. 2017). Dice loss takes both local and global loss information into account, which is essential for high accuracy. Unlike the cross-entropy loss, where the loss is determined as the average of per-pixel loss, and the per-pixel loss is discretely calculated without taking into account whether or not its neighboring pixels are borders. Cross entropy loss, which only takes into account loss in a micro sense instead of globally, is insufficient for image level prediction as a result. The Dice loss function is represented by the following:

$$D = \frac{2\sum_i^N PiGi}{\sum_i^N Pi^2 + \sum_i^N Gi^2} \qquad (1)$$

P_i and G_i are corresponding prediction and ground truth pixel values where these values in the boundary detection scenario are either 0 or 1, indicating whether the pixel is a boundary (1) or not (0). Since the sum increases only when Gi and P_i match, the numerator is the total of boundary pixels that were successfully predicted (both of value 1), whereas the denominator is the total of all boundary pixels from both the prediction and the ground truth.

3.5 CNN Classifier Architecture

The proposed CNN architecture which used for classifying breast tumor images is shown in Figure 3.5. The CNN architecture is made up of four convolutional layers where every convolutional layer has a distinct number of filters with the same size (3x3). The following are number of filters in the convolutional layers:

- 32 filters have been used in the first convolutional layer.
- 64 filters have been used in the second convolutional layer.
- 128 filters have been used filters in the third convolution layer.
- 256 filters have been used in the fourth convolutional layer.

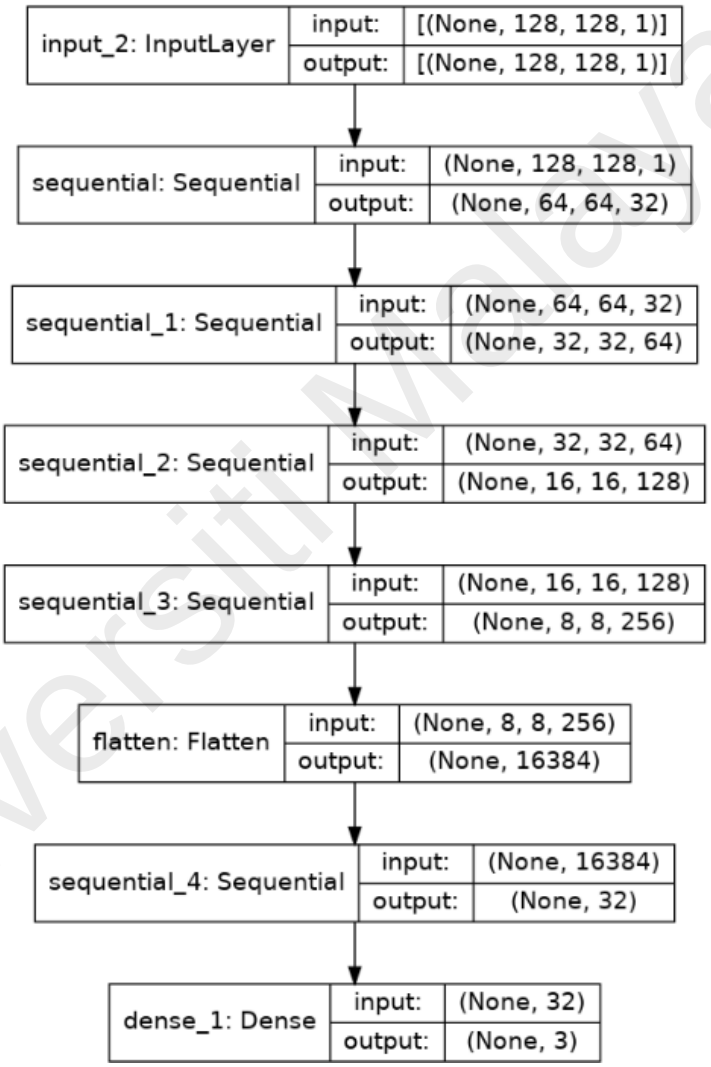

Figure 3.8: The CNN classifier model architecture

A zero-padding and a stride of 1 have been used in all convolutional processes. The LeakyReLU (Leaky Rectifier Linear Unit) function has been used as an activation

function for all convolutional layers. The use of the ReLU in deep neural networks has a number of benefits over other non-linear functions like the sigmoid because it lowers the probability of vanishing gradients and signifies a sparse representation for each layer which can enhance performance and speed up the learning process (Khan et al. 2018). A 2x2 max-pooling layer has been used after the LeakyReLU function has been applied. The max-pooling operation aims to reduce CNN dimensionality and increase input object position insensitivity. Lastly, there are two fully connected layers follow the fourth convolutional layer. A LeakyReLU and a softmax activation function are used with the 1st and 2nd fully connected layers where the LeakyReLU function provides nonlinearity and the softmax activation function yields a binary classification or a binary logistic regression with cross-entropy loss (Khan et al. 2018).

3.6 Software Implementation Tools

The following software has been used in order to develop the proposed model:

- **Kaggle**: is a Google LLC subsidiary, is a data scientist and machine learning user online community. Users can use Kaggle to search and upload datasets, investigate, and construct models in a web-based data-science environment, collaborate with other data scientists and machine learning experts, and compete to solve data science challenges.
- **TensorFlow**: an open-source and free machine learning and artificial intelligence software library. It can be used for a variety of applications, but it focuses on deep neural network training and inference. TensorFlow can be utilised with a broad range of programming languages, including Python, C++, and Javascript. This adaptability gives itself to a variety of applications in a variety of fields.

- **OpenCV**: a programming function library focused mostly at real-time computer vision.
- **NumPy**: an open-source Python library that adds support for wide, multi-dimensional arrays and matrices, as well as a wide variety of high-level mathematical operations to work on these arrays.
- **Sklearn:** a free machine learning software package for Python. It includes random forests, support-vector machines, k-means, gradient boosting, and DBSCAN as regression, classification, and clustering techniques, and is designed to work with the Python numeric and scientific libraries such as NumPy and SciPy.

CHAPTER 4: RESULTS AND DISCUSSION

4.1 Data Preparation

The collection of a well-defined dataset of ultrasound images is essential to the classification of breast lesions research. As a result, the publicly available BUID (Al-Dhabyani et al. 2020) is used in this project. The BUID includes 780 PNG greyscale images with an average image size of 500 x 500 pixels. The dataset is categorized into three groups: malignant, benign, and normal, with each image having its own mask image where the ground truth images matched by original images. There are 437 images in the benign, 133 in the normal, and 210 in the malignant classes. The Figure 4.1 shows the original images along with their mask images.

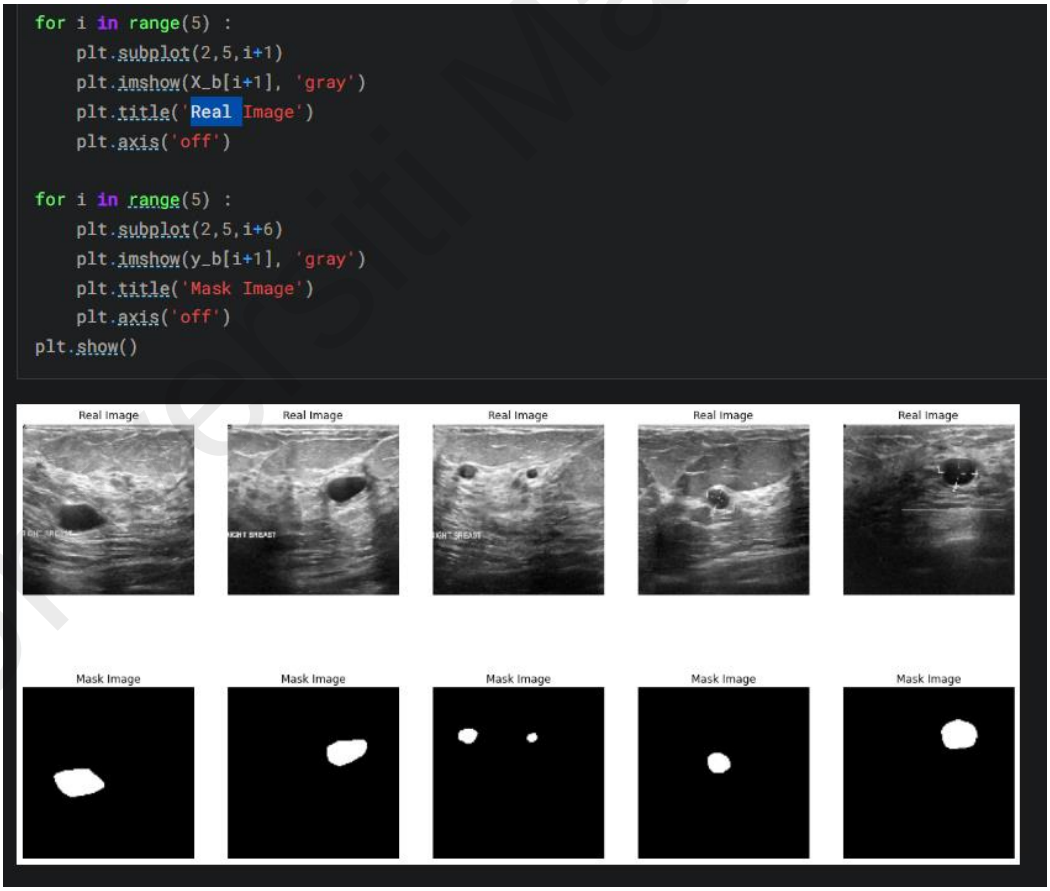

Figure 4.1: Visualization of original and mask images in BUID dataset

The BUID must be preprocessed before being used in the classification procedure. The most important stage of pre-processing is adjusting the dataset in such a manner that the original content of each image is preserved to the greatest extent possible while keeping the entire dataset constant in terms of image size. As a result, at the start of the project, all of the images were resampled to 128 × 128 pixels with a 95-5 train-test split for the U-Net model and 90-10 train-test split for the CNN classifier model.

The dataset has been split in order to perform fivefold cross-validation, with 90% of the dataset used for training and 10% for testing. By performing this procedure five times, choosing a different set each time as the testing set, it was assured that all of the subsets were used in both testing and training. Furthermore, image normalization was utilized, where the dataset was divided by 255 due to the presence of grayscale images. This has been done to increase the contrast of images with low contrast due to glare and to establish a consistent dynamic range throughout the datasets. Furthermore, data augmentation is used to improve model performance by preventing the neural network from learning irrelevant features due to the limited size of the training dataset. A function is defined in this project to do simple augmentation techniques such as rotation, flipping, zooming, and so on.

4.2 Implementation Details

After the dataset is prepared, the creation of the U-Net model has been established. U-Net has been used for localization because of its ability to locate and distinguish borders by performing classification on each pixel in the input image, producing input and output images that are the same size. As previously stated, the U-Net is divided into two paths: contracting and expanding. Therefore, firstly, the contracting path network is constructed as shown in Figure 4.2.

```
def conv2d_block(input_tensor, n_filters, kernel_size = 3, batchnorm = True):
    # first layer
    x = Conv2D(filters = n_filters, kernel_size = (kernel_size, kernel_size),\
               kernel_initializer = 'he_normal', padding = 'same')(input_tensor)
    if batchnorm:
        x = BatchNormalization()(x)
    x = Activation('relu')(x)

    # second layer
    x = Conv2D(filters = n_filters, kernel_size = (kernel_size, kernel_size),\
               kernel_initializer = 'he_normal', padding = 'same')(input_tensor)
    if batchnorm:
        x = BatchNormalization()(x)
    x = Activation('relu')(x)

    return x
```

+ Code + Markdown

```
def get_unet(input_img, n_filters = 16, dropout = 0.1, batchnorm = True):
    # Contracting Path
    c1 = conv2d_block(input_img, n_filters * 1, kernel_size = 3, batchnorm = batchnorm)
    p1 = MaxPooling2D((2, 2))(c1)
    p1 = Dropout(dropout)(p1)

    c2 = conv2d_block(p1, n_filters * 2, kernel_size = 3, batchnorm = batchnorm)
    p2 = MaxPooling2D((2, 2))(c2)
    p2 = Dropout(dropout)(p2)

    c3 = conv2d_block(p2, n_filters * 4, kernel_size = 3, batchnorm = batchnorm)
    p3 = MaxPooling2D((2, 2))(c3)
    p3 = Dropout(dropout)(p3)

    c4 = conv2d_block(p3, n_filters * 8, kernel_size = 3, batchnorm = batchnorm)
    p4 = MaxPooling2D((2, 2))(c4)
    p4 = Dropout(dropout)(p4)

    c5 = conv2d_block(p4, n_filters = n_filters * 16, kernel_size = 3, batchnorm = batchnorm)
```

Figure 4.2: Code for building the contracting path network

The network is made up of two 3 x 3 convolutional layers where each layer is followed by a 2 x2 max-pooling layer that has stride of 2 utilized for down sampling and one ReLU. Furthermore, the number of feature channels is doubled with each down sampling step. BatchNormalization has been added to the model to settle the learning process and reduce the number of training epochs. Next, the expanding path is constructed as shown in Figure 4.3.

```
    # Expansive Path
    u6 = Conv2DTranspose(n_filters * 8, (3, 3), strides = (2, 2), padding = 'same')(c5)
    u6 = concatenate([u6, c4])
    u6 = Dropout(dropout)(u6)
    c6 = conv2d_block(u6, n_filters * 8, kernel_size = 3, batchnorm = batchnorm)

    u7 = Conv2DTranspose(n_filters * 4, (3, 3), strides = (2, 2), padding = 'same')(c6)
    u7 = concatenate([u7, c3])
    u7 = Dropout(dropout)(u7)
    c7 = conv2d_block(u7, n_filters * 4, kernel_size = 3, batchnorm = batchnorm)

    u8 = Conv2DTranspose(n_filters * 2, (3, 3), strides = (2, 2), padding = 'same')(c7)
    u8 = concatenate([u8, c2])
    u8 = Dropout(dropout)(u8)
    c8 = conv2d_block(u8, n_filters * 2, kernel_size = 3, batchnorm = batchnorm)

    u9 = Conv2DTranspose(n_filters * 1, (3, 3), strides = (2, 2), padding = 'same')(c8)
    u9 = concatenate([u9, c1])
    u9 = Dropout(dropout)(u9)
    c9 = conv2d_block(u9, n_filters * 1, kernel_size = 3, batchnorm = batchnorm)
```

Figure 4.3: Code for building the expanding path network

The network consists of two 3x3 convolutions where every stage the feature map is upsampled and a 2x2 convolution layer is followed by to cut the feature channels numbers in half, then it is followed by a concatenation with the correspondingly cropped feature map from the contracting path, each followed by a ReLU. Cropping is necessary because to the loss of border pixels in each convolution. Finally, each 64-component feature vector is mapped to the required number of classes using a 1x1 convolution at the final layer.

Furthermore, the Adam gradient descent optimization algorithm has been applied with a learning rate of 0.00005 in order to help the model learn over time. Lastly, a loss function is used to assess how well the prediction model performs in terms of predicting the expected outcome. The loss function used to evaluate model performance in semantic segmentation is Dice loss function as shown in Figure 4.4.

```
def dice_coeff(y_true, y_pred):
    smooth = 1.
    # Flatten
    y_true_f = tf.reshape(y_true, [-1])
    y_pred_f = tf.reshape(y_pred, [-1])
    intersection = tf.reduce_sum(y_true_f * y_pred_f)
    score = (2. * intersection + smooth) / (tf.reduce_sum(y_true_f) + tf.reduce_sum(y_pred_f) + smooth)
    return score

def dice_loss(y_true, y_pred):
    loss = 1 - dice_coeff(y_true, y_pred)
    return loss

def bce_dice_loss(y_true, y_pred):
    loss = losses.binary_crossentropy(y_true, y_pred) + dice_loss(y_true, y_pred)
    return loss
```

Figure 4.4: Code for defining the Dice loss function

Next, a convolution neural network (CNN) is constructed in order to classify the generated mask images into benign, malignant or normal. The mask images in the BUID dataset, which is shown in Figure 4.5, is used for training the CNN classifier model. First,

the mask images are split into 90% for training and 10% for testing in order to perform fivefold cross-validation.

Despite the fact that there is an uneven distribution in the dataset, a model that performs well in classification tasks can be simply created due to significant distinctions between these images. In addition, because of the limited size of the generated mask images dataset, data augmentation is employed to improve model performance by helping the neural network to avoid learning irrelevant features. Therefore, a function is defined to do simple augmentation techniques like as rotation, flipping, zooming.

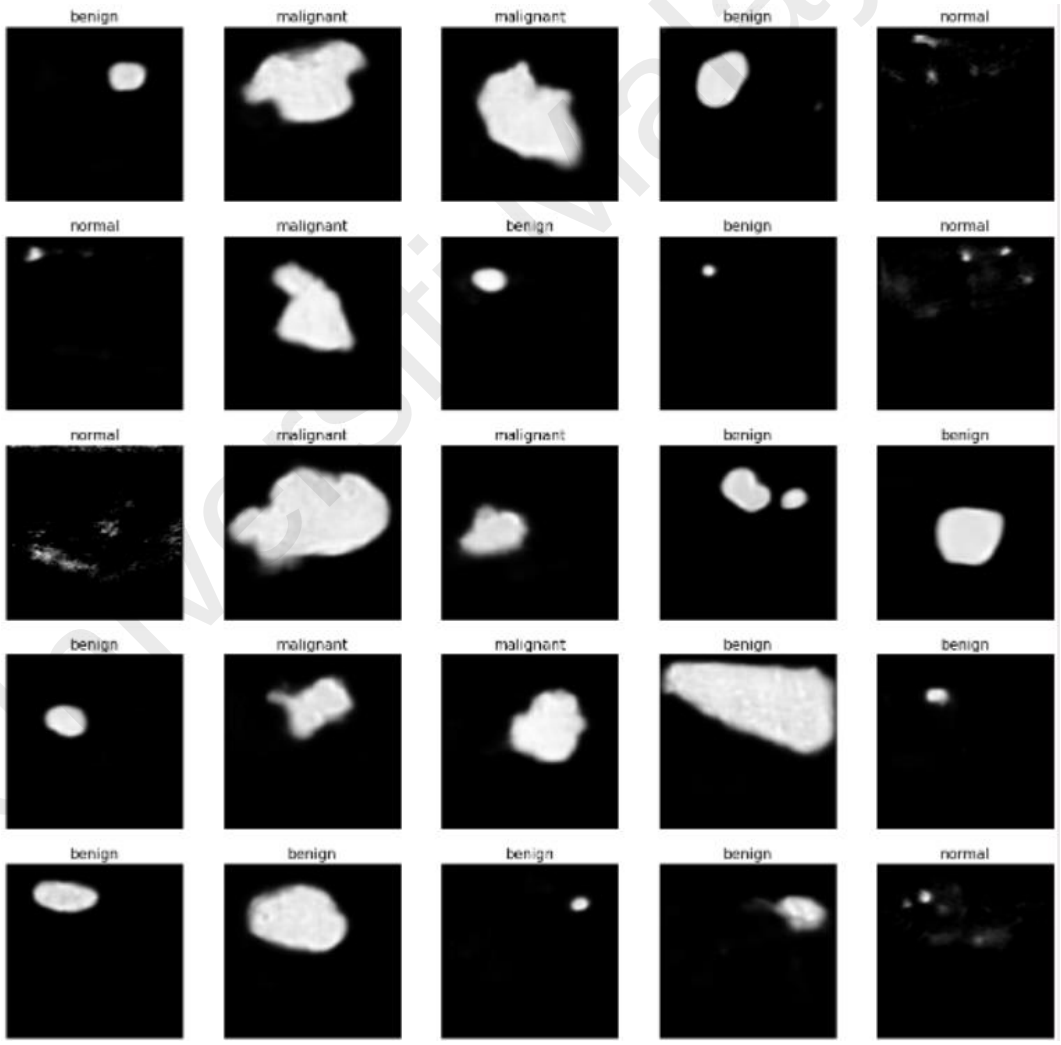

Figure 4.5: Random samples of mask images from the BUID dataset

Next, the construction of the CNN began by building of four convolutional layers where each convolutional layer has a distinct number of filters with the same size (3x3) as seen in Figure 4.6. In all convolutional layers, zero padding and a stride of 1 were employed. As an activation function for all convolutional layers, the LeakyReLU (Leaky Rectifier Linear Unit) function was utilized. In addition, a 2x2 max-pooling layer was used after using the LeakyReLU function. Following the fourth convolutional layer, two fully connected layers are added. With the first and second fully connected layers, a LeakyReLU and a softmax activation function are applied, where the LeakyReLU function provides nonlinearity and the softmax activation function generates a binary logistic regression with cross-entropy loss or a binary classification.

```
def conv_block (filterx) :

    model = Sequential()

    model.add(Conv2D(filterx, (3,3), strides = 1, padding = 'same', kernel_regularizer = 'l2'))
    model.add(BatchNormalization())
    model.add(Dropout(.2))
    model.add(LeakyReLU())

    model.add(MaxPooling2D())

    return model

def dens_block (hiddenx) :

    model = Sequential()

    model.add(Dense(hiddenx, kernel_regularizer = 'l2'))
    model.add(BatchNormalization())
    model.add(Dropout(.2))
    model.add(LeakyReLU())

    return model
```

```
def cnn (filter1, filter2, filter3, filter4, hidden1) :

    model = Sequential([

        Input((128,128,1,)),
        conv_block(filter1),
        conv_block(filter2),
        conv_block(filter3),
        conv_block(filter4),
        Flatten(),
        dens_block(hidden1),
        Dense(3, activation = 'softmax')
    ])

    model.compile(loss = 'categorical_crossentropy', optimizer = Adam(learning_rate = 0.0005), metrics = ['accuracy'])
```

Figure 4.6: Code for building the CNN classifier network

4.3 U-Net Model Results and Evaluation

In order to assess the performance of the U-Net model in localizing the breast tumors, the Dice loss function is used. A high loss number typically implies that the model is producing incorrect output, whereas a low loss value shows that the model contains less

errors. Training loss and validation loss over time are one of the most commonly used metric combinations. The training loss is a metric that measures how well a deep learning model fits the training data. Validation loss, on the other hand, is a metric used to evaluate the performance of a deep learning model on the validation set. As can be seen in Figure 4.7, the model produced low training and validation loss values (0.6774 and 0.6476 respectively) which indicates that were only few errors in the model.

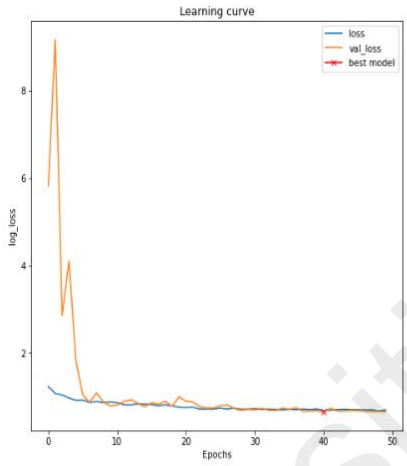

Evaluating the model on test sets

```
unet_model.load_weights('model-checkpoint.h5')
unet_model.evaluate(X_valid, y_valid, verbose=1)
```

```
5/5 [==============================] - 1s 37ms/step - loss: 0.6436 - dice_loss: 0.4391 - dice_coeff: 0.5609 - accuracy: 0.9285
[0.6435621976852417,
 0.43909239768981934,
 0.5609076023101807,
 0.9285187721252441]
```

Figure 4.7: The evaluation results of U-Net model

The validation loss and the training loss both decrease and stabilize at a certain point which indicates that the model has an optimal fit which means it does not underfit or overfit. In addition, the training accuracy and dice loss values achieved were 0.9285 and 0.4391 respectively, which indicates that the model performed very well, has high

accuracy, and have great ability in predicting mask images. Figure 4.8 illustrates the results of the U-Net model predicting the location of area which contains tumor growth. The first column shows the real medical images whereas the second column shows the ground truth mask images. The third column of images display the predicted mask images by the U-Net model.

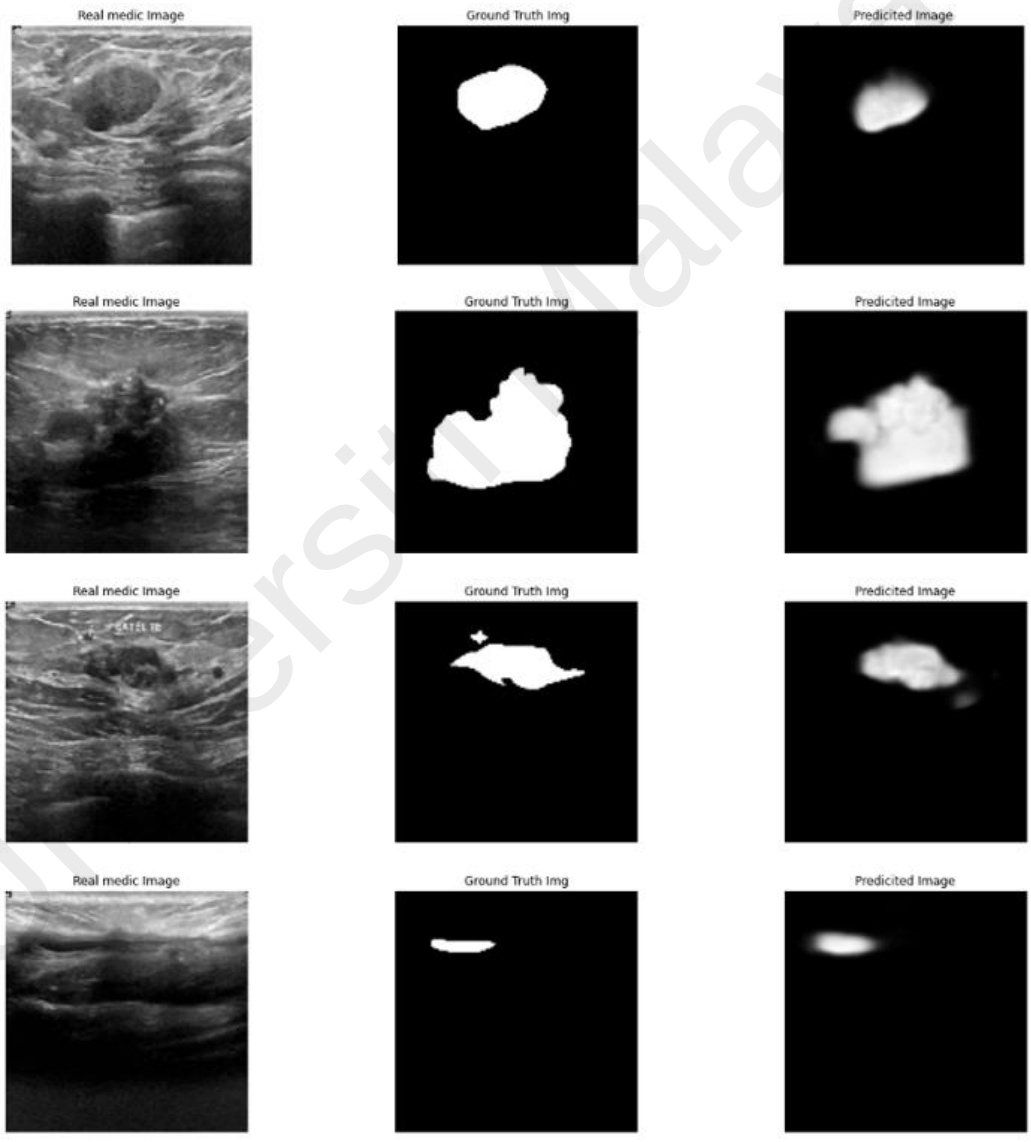

Figure 4.8: Results of U-Net predictions of breast tumor location

4.4 CNN Classifier Results and Evaluation

The proposed CNN model is evaluated to classify ultrasound breast images into malignant, benign, or normal based on the mask shape. In particular, accurate classification of malignant and benign lesions in ultrasound images is difficult due to artefacts such as shape variation, a low signal-to-noise ratio, ill-defined borders, and poor contrast. The resultant performance metrics of the proposed CNN model are shown in Figure 4.9.

```
print('Accuracy : ' + str(accuracy_score(y_test, y_pred)))
print(classification_report(y_test, y_pred, target_names = info))
```

```
Accuracy : 0.8461538461538461
              precision    recall  f1-score   support

      benign       0.86      0.86      0.86        42
      normal       0.94      1.00      0.97        16
   malignant       0.74      0.70      0.72        20

    accuracy                           0.85        78
   macro avg       0.85      0.85      0.85        78
weighted avg       0.84      0.85      0.84        78
```

Figure 4.9: Evaluation results of the CNN classifier model

From the Figure, it can be seen that the model achieved an accuracy equal to 0.85, and the precision of benign, malignant and normal images were 0.86, 0.74, and 0.94 respectively, demonstrating the classification ability and robust feature extraction of the proposed CNN model.

Accuracy is the most evident performance metric because it is simply the ratio of correctly predicted observations to total observations. Whereas precision is defined as the ratio of correctly predicted positive observations to all predicted positive observations. The ratio of accurately predicted positive observations to all observations in the actual class is referred to as recall. The F1 Score is calculated as the weighted average of

Precision and Recall. As a result, this score considers both false positives and false negatives.

In addition, a confusion matrix is applied in order to evaluate the performance of the CNN classification model on a set of test data for which the true values are known and to have a better understanding of what the CNN classification model achieves right and what types of errors it makes. A confusion matrix is simply a technique for summarizing a classification algorithm's performance. Figure 4.10 illustrates the confusion matrix for the proposed CNN classification model. As can be seen, almost all the actual target values match those predicted by the CNN classification model.

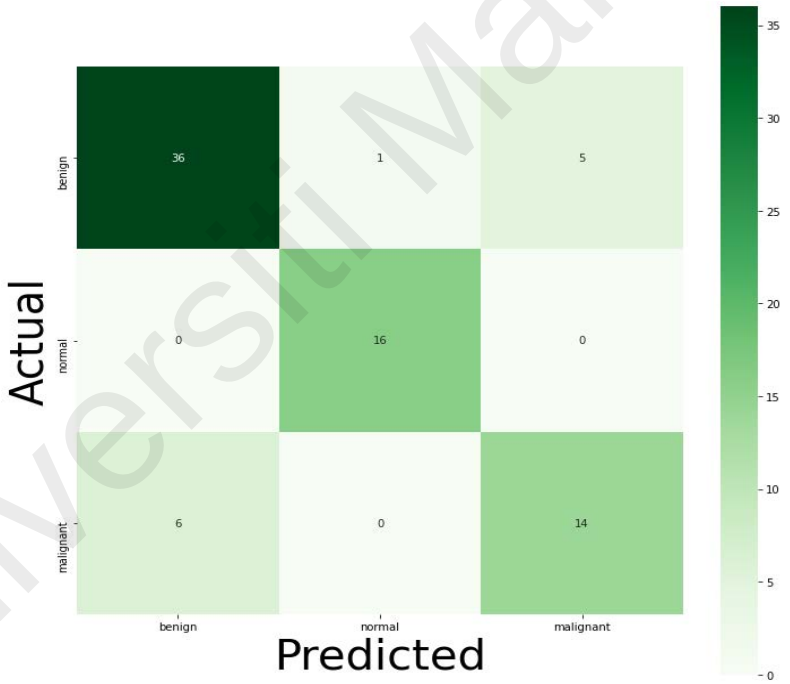

Figure 4.10: The confusion matrix results of the CNN classifier model

Lastly, the overall task is tested where the mask image is firstly predicted using the U-Net model and then based on the mask shape, the tumor is classified to either benign, malignant, or normal. Figure 4.11 illustrates the predicted results of the overall task using the two models.

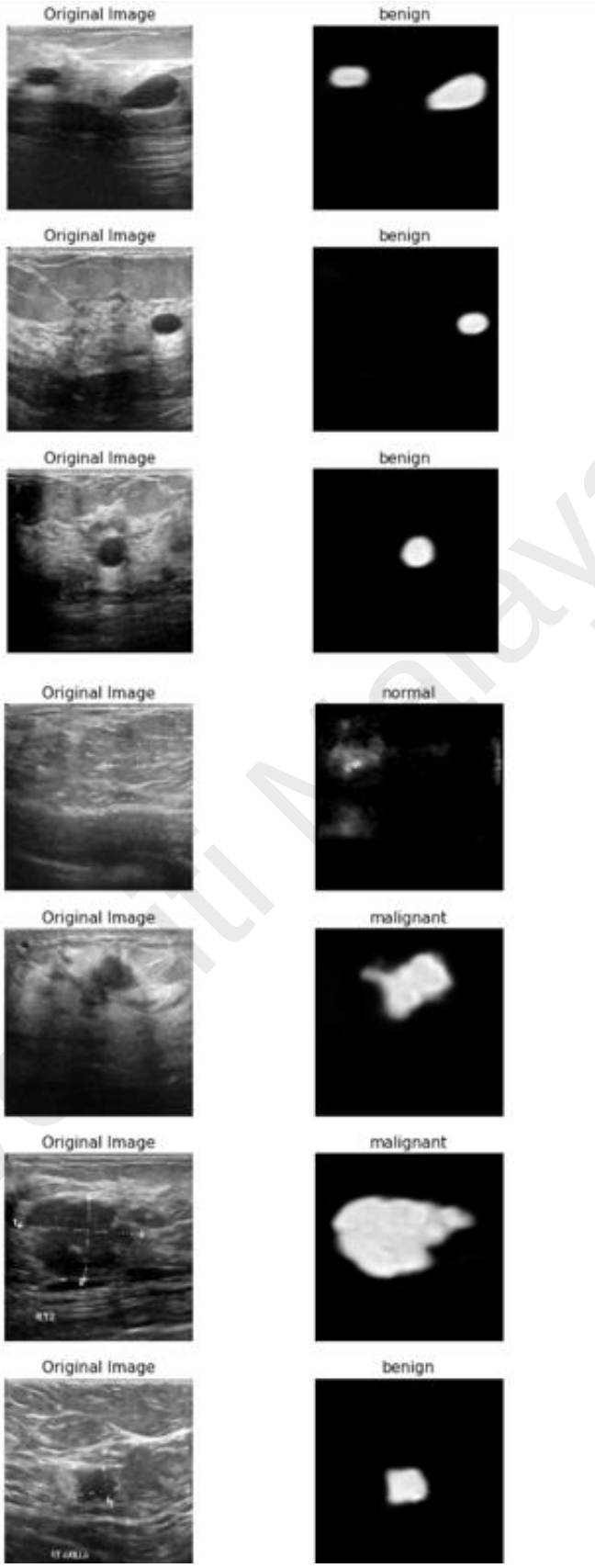

Figure 4.11: Results of classifying the generated mask images from the U-Net model.

The first column of displays the original medical images from the dataset, whereas the second column displays the predicted mask images labelled with its predicted classification using U-Net and CNN models. As can be seen from the figure, it is notable that proposed U-Net and CNN models produced great results with great accuracies.

CHAPTER 5: CONCLUSION

5.1 Conclusion

Because breast density has no effect on ultrasound waves in the breast, ultrasound imaging is considered a safe and effective procedure for women. However, contrary to MRI and mammography, conventional breast ultrasound is prone to uncertainty, which can result in a missed diagnosis and an unneeded biopsy. The ability of the radiologist is crucial for feature extraction in ultrasound imaging, a difficult and time-consuming activity that frequently depends on human intervention and demands for many pre-processing steps and leads to subject diagnosis. Therefore, in this research project, a detailed analysis and comparative review of existing and recent breast tumor classification algorithms has been carried out and the problems and gaps existed in previous approaches are identified. Then, a deep learning image classification model is proposed to classify breast tumors into benign, malignant, or normal. U-Net and CNN classifier model have been trained using the BUID dataset, where the dataset is prepared and preprocessed appropriately. Because of its ability to perform classification on each pixel in the input image and produce input and output images that are the same size, the U-Net model is used in this project to localize areas that contains tumor growth in the original medical images The generated mask images from the U-Net model are then classified using a CNN classifier model as benign, malignant, or normal. The Dice loss function and accuracy performance matrices are used to assess the performance of both U-Net and CNN classifier models. The evaluation results of both U-Net and CNN classifier models have shown a great capability of localizing and classifying breast tumors accurately.

5.2 Future work

Investigating other various CNN architectures is one of the future works. There is no doubt that some more effective networks will be offered in the near future given the acceleration of developments in this field. Generally, the innovation of CNN network architectures and the improvement of the network training method or optimization method benefits and improves image classification results.

A single classifier usually considered to be not sufficient, and therefore developing a strategy to combine or choose the classifiers based on an input image could improve accuracy. Because, to some extent, creating a monolithic classifier in order to cover all of the variability inherent in most pattern recognition problems is difficult.

REFERENCES

Akin, O., et al.: Advances in oncologic imaging: update on 5 common cancers. CA: Cancer J. Clin. 62(6), 364 (2012)

Al-Dhabyani W, Gomaa M, Khaled H, Fahmy A. Dataset of breast ultrasound images. Data in Brief. 2020 Feb;28:104863.

Alom, M.Z.; Yakopcic, C.; Nasrin, M.S.; Taha, T.M.; Asari, V.K. Breast Cancer Classification from Histopathological Images with

Amit G, Ben-Ari R, Hadad O, Monovich E, Granot N, Hashoul S (2017) Classification of breast MRI lesions using small-size training sets: comparison of deep learning approaches. Paper presented at the progress in biomedical optics and imaging—proceedings of SPIE

Amodei D, Ananthanarayanan S, Anubhai R, Bai J, Battenberg E, Case C et al (2016) Deep speech 2: endto-end speech recognition in English and mandarin. Paper presented at the International conference on machine learning

Araujo T, Aresta G, Castro E, Rouco J, Aguiar P, Eloy C et al (2017) Classification of breast cancer histology images using convolutional neural networks. PLoS ONE 12(6):14.

Asri, H.; Mousannif, H.; Moatassime, H.A.; Noel, T. Using Machine Learning Algorithms for Breast Cancer Risk Prediction and Diagnosis. Procedia Comput. Sci. 2016, 83, 1064–1069.

Bakkouri I, Afdel K (2017) Breast tumor classification based on deep convolutional neural networks. Paper presented at the Proceedings—3rd international conference on advanced technologies for signal and image processing, ATSIP 2017

Bevilacqua V, Brunetti A, Triggiani M, Magaletti D, Telegrafo M, Moschetta M (2016) An optimized feedforward artificial neural network topology to support radiologists in breast lesions classification. Paper presented at the GECCO 2016 companion—proceedings of the 2016 genetic and evolutionary computation conference

Byra M, Piotrzkowska-Wroblewska H, Dobruch-Sobczak K, Nowicki A (2017) Combining Nakagami imaging and convolutional neural network for breast lesion classification. Paper presented at the IEEE international ultrasonics symposium, IUS

Byra, M.; Galperin, M.; Ojeda-Fournier. H.; Comstock, C.; Andre. M.: Breast mass classification in sonography with transfer learning using a deep convolutional neural network and colour conversion, Med. Phys., vol. 46, no. 2, 2019.

Byra, M.; Nowicki, A.; Wróblewska-Piotrzkowska, H.; Dobruch-Sobczak, K. Classification of breast lesions using segmented quantitative ultrasound maps of homodyned K distribution parameters. Med. Phys. 2016, 43, 5561–5569.

Carneiro G, Nascimento J, Bradley AP (2017) Automated analysis of unregistered multi-view mammograms with deep learning. IEEE Trans Med Imaging 36(11):2355–2365.

Carole H Sudre, Wenqi Li, Tom Vercauteren, Sebastien Ourselin, and M Jorge Cardoso. Generalised dice overlap as a deep learning loss function for highly unbalanced segmentations. In Deep learning in medical image analysis and multimodal learning for clinical decision support, pages 240–248. Springer, 2017.

Cheng J-Z, Ni D, Chou Y-H, Qin J, Tiu C-M, Chang Y-C et al (2016) Computer-aided diagnosis with deep learning architecture: applications to breast lesions in US images and pulmonary nodules in CT scans. Sci Rep 6:24454.

Cheng, H.D., Shan, J., Ju, W., Guo, Y.H., Zhang, L.: Automated breast cancer detection and classification using ultrasound images: a survey. Pattern Recogn. 43, 299–317 (2010) computer-aided diagnosis: differences in lesions presenting as mass and non-mass-like enhancement. Eur. Radiol. 20, 771–781 (2010).

D. J. Dronkers, J. H. C. L. Hendriks, R. Holland, G. Rosenbusch, eds. Practice of mammography: pathology – technique – interpretation – adjunct modalities. New York: Tyeme Verlag, 2002.

Dhungel N, Carneiro G, Bradley AP (2017) A deep learning approach for the analysis of masses in mammograms with minimal user intervention. Med Image Anal 37:114–128.

Duraisamy S, Emperumal S (2017) Computer-aided mammogram diagnosis system using deep learning convolutional fully complex-valued relaxation neural network classifier. IET Comput Vision 11(8):656–662.

Eisenbrey, J.R.; Dave, J.K.; Forsberg, F. Recent technological advancements in breast ultrasound. Ultrasonics 2016, 70, 183–190.

Fujita, H. AI-Based Computer-Aided Diagnosis (AI-CAD): The Latest Review to Read First. Radiol. Phys. Technol. 2020, 13, 6–19.

Goceri E (2018) Formulas behind deep learning success. Paper presented at the international conference on applied analysis and mathematical modeling. Istanbul, Turkey

Han Z, Wei B, Zheng Y, Yin Y, Li K, Li S (2017) Breast cancer multi-classification from histopathological images with structured deep learning model. Sci Rep.

Hijab, A.; Rushdi, M.; Gomaa, M.; Eldeib, A.: Breast cancer classification in ultrasound images using transfer learning, IEEE fifth inrenational conference on advances in biomedical engineering, 2019

Huang, Q.; Hu, B.; Zhang, F. Evolutionary optimized fuzzy reasoning with mined diagnostic patterns for classification of breast tumors in ultrasound. Inf. Sci. 2019, 502, 525–536 Inception Recurrent Residual Convolutional Neural Network. J. Digit. Imaging 2019, 32, 605–617.

J. Ferlay, I. Soerjomataram, M. Ervik, R. Dikshit, S. Eser, C. Mathers, M. Rebelo, D. Parkin, D. Forman, F. Bray. GLOBOCAN 2012 v1.0, Cancer Incidence and Mortality Worldwide: IARC CancerBase No. 11. Tech. rep. 11. Lyon: International Agency for Research on Cancer, Jan. 2013. url: http://globocan.iarc.fr

James JJ, Wilson ARM, Evans AJ (2016) The breast. Retrieved from https://radiologykey.com/the-breast-2/. Jan. 2013. url: http://www.wcrf.org/cancer_statistics/world_cancer_ statistics.php.

Khairi SSM, Bakar MAA, Alias MA, Bakar SA, Liong CY, Rosli N, Farid M. Deep Learning on Histopathology Images for Breast Cancer Classification: A Bibliometric Analysis. Healthcare (Basel). 2021 Dec 22;10(1):10.

Khan S.; Rahmani H.; Shah, S. A. A.: A Guide to Convolutional Neural Networks for Computer Vision, Morgan & Claypool Publishers, Synthesis Lectures on Computer Vision, ISBN-10: 1681730219, 2018

Kharya, S.; Agrawal, S.; Soni, S. Naive Bayes Classifiers: A Probabilistic Detection Model for Breast Cancer. Int. J. Comput. Appl. 2014, 92, 26–31.

Kiambe, K.; Kiambe, K. Breast Histopathological Image Feature Extraction with Convolutional Neural Networks for Classification. ICSES Trans. Image Process. Pattern Recognit. (ITIPPR) 2018, 4, 4–12.

Kim DH, Kim ST, Ro YM (2016) Latent feature representation with 3-D multi-view deep convolutional neural network for bilateral analysis in digital breast tomosynthesis. Paper presented at the 2016 IEEE international conference on acoustics, speech and signal processing (ICASSP)

Komura, D.; Ishikawa, S. Machine Learning Methods for Histopathological Image Analysis. Comput. Struct. Biotechnol. J. 2018, 16, 34–42.

Kumar D, Kumar C, Shao M (2017) Cross-database mammographic image analysis through unsupervised domain adaptation. Paper presented at the 2017 IEEE international conference on big data (big data)

Lakhani P, Sundaram B (2017) Deep learning at chest radiography: automated classification of pulmonary tuberculosis by using convolutional neural networks. Radiology 284(2):574–582

LeCun, Y.; Bengio, Y.; Hinton, G. Deep Learning. Nature 2015, 521, 436–444.

Liu F, Hernandez-Cabronero M, Sanchez V, Marcellin MW, Bilgin A (2017) The current role of image compression standards in medical imaging. Information 8(4):131

MFMER (2018) Breast MRI. Retrieved from https://www.mayoclinic.org/tests-procedures/breast-mri/about/ pac-20384809.

Moon M, Cornfeld D, Weinreb J (2009) Dynamic contrast-enhanced breast MR imaging. Magn Reson Imaging Clin N Am 17(2):351–362

Murtaza, Ghulam & Shuib, Liyana & Wahid, Ainuddin & Mujtaba, Ghulam & Nweke, Henry & Al-Garadi, Mohammed & Zulfiqar, Fariha & Raza, Ghulam & Azmi, Nor. (2020). Deep learning-based breast cancer classification through medical imaging modalities: state of the art and research challenges. Artificial Intelligence Review. 53. 10.1007/s10462-019-09716-5.

Nascimento CDL, Silva SDS, da Silva TA, Pereira WCA, Costa MGF, Costa Filho CFF (2016) Breast tumor classification in ultrasound images using support vector machines and neural networks. Revista Brasileira de Engenharia Biomedica 32(3):283–292.

Newell, D. et al. Selection of diagnostic features on breast MRI to differentiate between malignant and benign lesions using

Octaviani, T.L.; Rustam, Z. Random Forest for Breast Cancer Prediction. In Proceedings of the AIP Conference Proceedings, Depok, Indonesia, 30–31 October 2018; pp. 1–7.

Pal, K. K.; Sudeep, K. S.: Preprocessing for Image Classification by Convolutional Neural Networks. International Conference on Trends in Electronics Information Communication Technology, pp. 1778– 1781 (2016).

Parkhi OM, Vedaldi A, Zisserman A (2015) Deep face recognition. Paper presented at the BMVC

Piotrzkowska-Wroblewska, H.; Dobruch-Sobczak, K.; Litniewski, J.; Chrapowicki, E.; Roszkowska-Purska, K.; Nowicki, A. Differentiation of the breast lesions using statistics of backscattered echoes. Hydroacoustics 2016, 19, 319–328.

Qiu Y, Yan S, Gundreddy RR, Wang Y, Cheng S, Liu H, Zheng B (2017) A new approach to develop computeraided diagnosis scheme of breast mass classification using deep learning technology. J X-Ray Sci Technol 25(5):751–763.

Qu, X.X.; Song, Y.; Zhang, Y.H.; Qing, H.M. Value of ultrasonic elastography and conventional ultrasonography in the differential diagnosis of non-mass-like breast lesions. Ultrasound Med. Biol. 2019, 45, 1358–1366.

Rasti R, Teshnehlab M, Phung SL (2017) Breast cancer diagnosis in DCE-MRI using mixture ensemble of convolutional neural networks. Pattern Recogn 72:381–390.

Rezaeilouyeh, H.; Mollahosseini, A.; Mahoor, M.H. Microscopic Medical Image Classification Framework via Deep Learning and Shearlet Transform. J. Med. Imaging 2016, 3, 044501.

Rezaeilouyeh, H.; Mollahosseini, A.; Mahoor, M.H. Microscopic Medical Image Classification Framework via Deep Learning and Shearlet Transform. J. Med. Imaging 2016, 3, 044501.

Ronneberger, O., Fischer, P., Brox, T. (2015). U-Net: Convolutional Networks for Biomedical Image Segmentation. In: Navab, N., Hornegger, J., Wells, W., Frangi, A. (eds) Medical Image Computing and Computer-Assisted Intervention – MICCAI 2015. MICCAI 2015. Lecture Notes in Computer Science(), vol 9351.

Rubin R, Strayer DS, Rubin E (2008) Rubin's pathology: clinicopathologic foundations ofmedicine. Lippincott Williams & Wilkins, Philadelphia

Sakr, G. E.; Mokbel, M.; Darwich, A.; Khneisser, M. N.; Hadi, A.: Comparing deep learning and support vector machines for autonomous waste sorting, IEEE International Multidisciplinary Conference on Engineering Technology (IMCET), Beirut, pp. 207- 212, 2016.

Samala RK, Chan HP, Hadjiiski LM, Helvie MA, Richter C, Cha K (2018) Evolutionary pruning of transfer learned deep convolutional neural network for breast cancer diagnosis in digital breast tomosynthesis. Phys Med Biol 63(9):8

Siegel, R.L., Miller, K.D., Jemal, A.: Cancer statics, 2017. CA Cancer J. Clin. 67(1), 7–30 (2017)

Singh, S., Maxwell, J., Baker, J. A., Nicholas, J. L. & Lo, J. Y. Computer-aided classification of breast masses: performance and interobserver variability of expert radiologists versus residents. Radiology 258, 73–80 (2011)

Singh, V.K.; Abdel-Nasser, M.; Akram, F.; Rashwan, H.A.; Sarker, M.K.; Pandey, N.; Romani, S.; Puig, D. Breast tumor segmentation in ultrasound images using contextual-information-aware deep adversarial learning framework. Expert Syst. Appl. 2020, 162, 113870

Stavros, A., Thickman, D., Rapp, C., Dennis, M., Parker, S., Sisney, G.: Solid breast nodules: use of sonography to distinguish between benign and malignant lesions. Radiology 196(1), 123– 134 (1995)

Svozil D, Kvasnicka V, Pospichal J (1997) Introduction to multi-layer feed-forward neural networks. Chemometr Intell Lab Syst 39(1):43–62

Tessa S, Keith JFM (2018) The difference between an MRI and CT scan. Retrieved from https://www. healthline.com/health/ct-scan-vs-mri.

Tsui P-H, Ho M-C, Tai D-I, Lin Y-H, Wang C-Y, Ma H-Y (2016) Acoustic structure quantification by using ultrasound Nakagami imaging for assessing liver fibrosis.

Wang, H.; Cruz-Roa, A.; Basavanhally, A.; Gilmore, H.; Shih, N.; Feldman, M.; Tomaszewski, J.; Gonzalez, F.; Madabhushi, A. Mitosis Detection in Breast Cancer Pathology Images by Combining Handcrafted and Convolutional Neural Network Features. J. Med. Imaging 2014, 1, 034003.

Wang, Y. I.; Choi, E. J.; Choi, Y.; Zhang, H.; Jin, G. Y. and Ko, S. B.: Breast cancer classification in automated breast ultrasound using multiview convolutional neural network with transfer learning, Ultrasound in Med. & Biol., vol. 46, no. 5, pp. 1119-1132, 2020.

World Cancer Research Found International (WCRF). Worldwide Cancer Statistics.

World Health Organization (2018) Cancer. Retrieved from http://www.who.int/en/news-room/fact-sheets/ detail/cancer. Accessed 20 Sep 2018

Youk JH, Gweon HM, Son EJ (2017) Shear-wave elastography in breast ultrasonography: the state of the art. Ultrasonography 36(4):300–309.

Zhang Q, Xiao Y, Dai W, Suo JF, Wang CZ, Shi J, Zheng HR (2016) Deep learning-based classification of breast tumors with shear-wave elastography. Ultrasonics 72:150–157.

Zhou, S. K.; Greenspan, H.; Shen, D.: Deep learning for medical image analysis. First Edition, Elsevier, USA, 2017.

Zuluaga-Gomez, J.; Al Masry, Z.; Benaggoune, K.; Meraghni, S.; Zerhouni, N. A CNN-Based Methodology for Breast Cancer Diagnosis Using Thermal Images. Comput. Methods Biomech. Biomed. Eng. Imaging Vis. 2021, 9, 131–145.